Original Paper

Cells Tissues Organs

Cells Tissues Organs 2005;180:215–236
DOI: 10.1159/000088938

Accepted after revision: August 18, 2005

Spatial Distribution of Osteocyte Lacunae in Equine Radii and Third Metacarpals: Considerations for Cellular Communication, Microdamage Detection and Metabolism

John G. Skedros[a, b] Todd R. Grunander[a] Mark W. Hamrick[c]

[a]Department of Orthopaedic Surgery, University of Utah, [b]Department of Veteran's Affairs Medical Center, Bone and Joint Research Laboratory, Salt Lake City, Utah, and [c]Medical College of Georgia, Augusta, Ga., USA

Key Words
Equine bone · Osteocyte lacunae · Third metacarpal

Abstract
Osteocytes, which are embedded in bone matrix, are the most abundant cells in bone. Despite the ideal location of osteocytes to sense the local environment and influence bone remodeling, their functions, and the relative importance of these functions, remain controversial. In this study, we tested several hypotheses that address the possibilities that population densities of osteocyte lacunae (Ot.Lc.N/B.Ar) correlate with strain-, remodeling- or metabolism-related aspects of the local biomechanical environments of mid-third diaphyseal equine radii and third metacarpals from skeletally mature animals. Ot.Lc.N/B.Ar data, quantified in multiple cortical locations, were analyzed for possible correlations with (1) structural and material characteristics (e.g., cortical thickness, percent ash, secondary osteon population density, mean osteon cross-sectional area, and predominant collagen fiber orientation), (2) strain characteristics, including prevalent/predominant strain magnitude and mode (tension, compression, shear), (3) hypothesized strain-mode-related microdamage characteristics, which might be perceived by osteocyte 'operational' networks, and (4) variations in remodeling dynamics and/or metabolism (i.e. presumably higher in endocortical regions than in other transcortical locations). Results showed relatively uniform Ot.Lc.N/B.Ar between regions with highly non-uniform strain and strain-related environments and markedly heterogeneous structural and material organization. These results suggest that population densities of these cells are poorly correlated with mechanobiological characteristics, including local variations in metabolic rate and strain magnitude/mode. Although osteocytes hypothetically evolved both as strain sensors and fatigue damage sensors able to direct the removal of damage as needed, the mechanisms that govern the distribution of these cells remain unclear. The results of this study provide little or no evidence that the number of osteocyte lacunae has a functional role in mechanotransduction pathways that are typically considered in bone adaptation.

Abbreviations used in this paper

Ca	Calcium
CFO	Predominant collagen fiber orientation
Cd	Caudal
Cr	Cranial
Lc-Lc	Lacuna-lacuna distance
MC3	Third metacarpal
On.Ar	Osteon area
On.Ar/T.Ar	Fractional area of secondary osteonal bone
On.N/T.Ar	Secondary osteon population density
Ot.Lc.N/B.Ar	Osteocyte lacuna population density

KARGER

Fax +41 61 306 12 34
E-Mail karger@karger.ch
www.karger.com

1422–6405/05/1804–0215$22.00/0

Accessible online at:
www.karger.com/cto

Dr. John G. Skedros, MD
Utah Bone and Joint Center
5323 South Woodrow Street, Suite 202
Salt Lake City, UT 84107 (USA)
Tel. +1 801 713 0606, Fax +1 801 713 0609, E-Mail jskedros@utahboneandjoint.com

Introduction

Osteocytes, which are embedded in bone matrix, are by far the most abundant cells in bone. Their cell bodies are located in lacunae (ellipsoid cavities) and are extensively connected to one another as well as to bone-forming cells (osteoblasts) and bone-lining cells by cytoplasmic processes (dendrites) that radiate and ramify within canaliculi [Doty, 1981; Marotti, 1996; Ferretti et al., 1999]. Despite the ideal location of osteocytes to sense the local environment, their functions, and the relative importance of these functions, remain controversial. The multifactorial functions of osteocytes and the lacunocanalicular spaces in which they reside may include (1) mineral homeostasis [Aarden et al., 1994; Mullender et al., 1996b; Ehrlich et al., 2002; Knothe Tate, 2003; Parfitt, 2003; Tazawa et al., 2004], (2) nutrient transport and signal transmission [Starkebaum, 1979; Kelly, 1983; Lanyon, 1993; Marotti, 2000; Yellowley et al., 2000; Alford et al., 2003; Mishra and Knothe Tate, 2003], (3) mechanosensation/mechanotransduction [Cowin et al., 1991; Duncan and Turner, 1995; Mosley and Lanyon, 1998; Burger and Klein-Nulend, 1999; Weinbaum et al., 2001; Rubinacci et al., 2002], (4) microdamage detection [Mori and Burr, 1993; Bentolila et al., 1998; Martin, 2000; Reilly, 2000; Vashishth et al., 2000; Noble et al., 2003], and (5) the control of processes that mediate some bone remodeling and modeling activities, as well as the attainment of bone mass [Carter, 1987; Butler, 1989; Mullender and Huiskes, 1995; Terai et al., 1999; Martin, 2000; Power et al., 2002; Vashishth et al., 2002; Burger et al., 2003]. These interrelated functions may be mediated by intercellular communication via gap junctions or cellular activation resulting from interstitial fluid flow. For example, there is evidence that osteocyte cellular networks are sensitized to load-induced signals by low-level electromagnetic fields, which are produced by ion flow through intercellular gap junctions [Donahue, 1998, 2000; Yellowley et al., 2000]. These and other functions of this syncytium are probably influenced by variations in osteocyte densities [Marotti, 1996; Vashishth et al., 2000; Mishra and Knothe Tate, 2003].

Extending the work of Marotti et al. [1990] and Marotti [1996, 2000], Martin [2000] has suggested that osteocytes form a network that represses osteon-remodeling activity as governed by the local strain environment. This repression is removed when changes in the strain environment sufficiently perturb the cellular network (e.g., microdamage or limb immobilization). This hypothesized repressive function is also directly correlated with cell density [Metz et al., 2003]. In computation analyses, several investigators have suggested that osteocytes function as sensors of strain or strain-related stimuli (e.g., fluid flow and cell deformation), which can be upregulated in a cell density-dependent manner [Cowin et al., 1991; Weinbaum et al., 1994; Mullender and Huiskes, 1997; Carter and Beaupré, 2001]. For example, Mullender and Huiskes [1997] and Huiskes [2000] suggest that osteocytes, after receiving mechanical signals in the form of predominant strains, can regulate the activity of nearby basic multicellular units (i.e. the osteoclasts/osteoblasts of forming secondary osteons). Using a finite element model of a forming basic multicellular unit, Burger et al. [2003] also suggest that osteocyte-mediated activation of basic multicellular units might be a strain-regulated phenomenon influenced by osteocyte density. If osteocytes have important mechanosensory functions and influence osteon formation, and if these functions are influenced by their densities and governed by strain-related stimuli, then these 'sensors' might have different densities in regions exposed to different strain environments. Osteocytes might also be more numerous in bone with higher renewal rates [Canè et al., 1982; Power et al., 2002] or metabolism [Mullender et al., 1996a; Cullinane, 2002].

In order to further evaluate relationships between osteocyte populations and habitual strain environments, regional metabolism or remodeling dynamics, cellular communication, and microdamage detection, it is useful to examine their densities in bones with well-described strain environments such as equine radii and third metacarpals (MC3s). These bones experience predictable bending at mid-diaphysis, which results in opposing cortical regions being loaded in prevalent/predominant tension and compression [Schneider et al., 1982; Gross et al., 1992; Mason et al., 1995; Skedros et al., 1996] (fig. 1). In these habitual bending environments, compression locations typically receive relatively high magnitude strains, while neutral axis and endocortical regions (i.e. near the medullary canal) typically receive relatively low magnitude longitudinal strains. The low strain magnitudes, increased vascularity and proximity of endocortical regions to marrow may also influence their increased remodeling activity [Skedros et al., 1994b, 1996; Frost, 1998; Martin, 2000; Parfitt, 2001]. Neutral axis regions experience the highest strain gradients and highest directional fluid flow [Judex et al., 1997a], in addition to prevalent shear strains and principal (maximum) strains that are notably oblique to the longitudinal axis of the bone.

These non-uniform strain, fluid flow and remodeling environments can be associated with regional differences

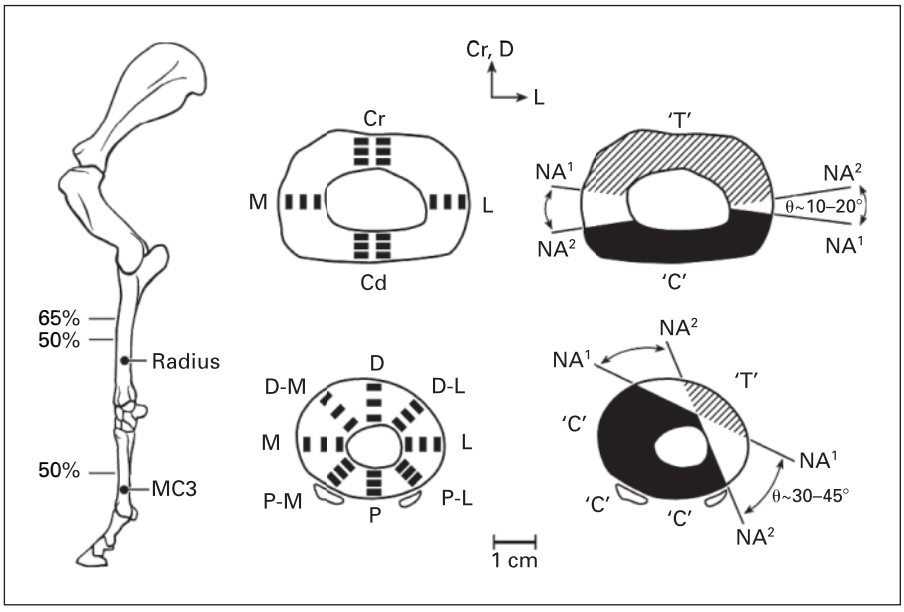

Fig. 1. Lateral view of a forelimb skeleton of a horse showing the radius and MC3. At near right: cross-sections showing image locations; at far right: approximate typical ranges subtended by the neutral axes (NA) during weight bearing. Changes in neutral axis locations for the equine MC3 are considered in tables 1 and 2 as two 'tension' regions and four 'compression' regions. 'C' = Compression region (darkened); 'T' = tension region (oblique lines); M = medial; L = lateral; D = dorsal; P = palmar; D-M = dorsal-medial; D-L = dorsal-lateral; P-M = palmar-medial; P-L = palmar-lateral.

in bone material organization or composition (e.g., predominant collagen fiber orientation (CFO), secondary osteon population density (On.N/T.Ar), secondary osteon 'types' (e.g., lamellar vs. parallel-fibered) [Marotti, 1996], mean osteon cross-sectional area, and percent ash). Some of these characteristics may be adaptations for the regionally prevalent/predominant strain mode (tension, compression or shear), magnitude or other strain-related characteristics. For example, cortices loaded habitually in compression tend to have greater On.N/T.Ar and/or more oblique-to-transverse CFO than opposing tension cortices [Marotti, 1963; Lanyon and Bourn, 1979; Bouvier and Hylander, 1981; Portigliatti Barbos et al., 1984; Skedros, 1994a; Mason et al., 1995; Skedros et al., 1996, 1997; Takano et al., 1999; Skedros, 2001a; Skedros et al., 2001b, 2001c; Kalmey and Lovejoy, 2002]. In turn, if specific strain characteristics are important determinants of bone remodeling and if osteocyte densities influence remodeling, then osteocyte densities might be correlated with osteon-mediated material characteristics, e.g., CFO, On.N/T.Ar, fractional area of secondary osteonal bone (On.Ar/T.Ar), osteon area (On.Ar), porosity from osteon canals, and percent ash from changes in mean tissue age associated with frequencies of young osteons. Osteocyte densities might therefore be useful for interpreting loading history.

In this study, we quantified differences in osteocyte lacuna population densities (Ot.Lc.N/B.Ar; n/mm^2) between cortices (dorsal, palmar, etc.) and transcortical 'regions' (pericortical, middle cortical, endocortical) and compared them with our previously published data correlating structural, material and strain characteristics in equine radii and MC3s [Mason et al., 1995; Skedros et al., 1996]. The strain characteristics include regional variations in strain magnitude and mode, and consider neutral axis locations, marrow proximity and remodeling activity. A mean distance between neighboring osteocyte lacunae and spatial heterogeneity of Ot.Lc.N/B.Ar for each location was estimated as well, in order to identify differences in their distribution. The data are also considered in the context of a literature review regarding important putative functions that osteocytes have in limb bone cortices. The hypotheses tested include the following:

1 Osteocyte lacuna densities will correlate with areas habitually loaded in compression due to the typically higher strains or other strain or strain-related characteristics, more predominantly oblique-to-transverse collagen fibers and/or higher On.N/T.Ar.
2 Osteocyte lacuna densities will correlate with proximity to marrow (i.e. endocortical regions), which experience relatively low strain and relatively higher remodeling/metabolic activity than other regions.
3 Osteocyte lacuna densities will exhibit differences in 'tension', 'compression' and 'neutral axis' cortices, possibly satisfying different regional, 'sensor' requirements for detecting strain-mode-related differences in microdamage incidence and/or size (e.g., smaller-sized

microcracks in habitual tension environments compared with habitual compression environments).

4 Spatial heterogeneity of osteocyte lacunae will exhibit correlations with On.Ar/T.Ar and/or with strain mode variations as a function of the prevalence of specific secondary osteon 'types' (i.e. parallel-fibered secondary osteons vs. lamellar secondary osteons).

Materials and Methods

Ten radii and nine MC3s were obtained from skeletally mature Standardbred horses with no evidence of skeletal pathology at the time of death and no history of racing or race training. The bones had been used in previous studies that reported correlations of various material characteristics with their habitual strain environments from the mid-diaphysis (MC3) or from the middle third of the diaphysis (radius; two sectioned locations) [Mason et al., 1995; Skedros et al., 1996]. The radii were randomly selected from 10 horses and the MC3s from 9 horses, resulting in an approximately even number of left and right bones. Each bone was manually cleaned of soft tissue and then sectioned transversely at the 50% (MC3) or 50 and 65% of its length (radius). One 5-mm-thick segment was cut immediately distal to each of these transection levels. The segments were embedded (undemineralized, unstained) in polymethyl methacrylate [Emmanual et al., 1987] and prepared for backscattered electron imaging in the scanning electron microscope [Skedros et al., 1993a, 1993b; Bloebaum et al., 1997].

In the MC3s, one 50× high-resolution backscattered electron micrograph (1.6 × 2.3 mm) was taken within each of the three transcortical 'envelopes' or 'regions' (i.e. pericortical, middle cortical and endocortical) in octant locations: dorsal, dorsal-lateral, lateral, palmar-lateral, palmar, palmar-medial, medial and dorsal-medial, for a total of 24 image locations (fig. 1). In the radii, two 50× high-resolution backscattered electron micrographs (2.71 × 2.71 mm) were taken within each of the three regions of the cranial (Cr) and caudal (Cd) cortices, and one image in each region of the medial and lateral cortices for a total of 12 image locations in each section. Micrographs were developed on Polaroid™ film.

Osteocyte lacunae were manually counted by trained technicians and confirmed by the principal investigator who independently analyzed a subset of images. The images were randomly assorted and the technicians were blinded to cortical location and to the hypotheses of the study. Inter- and intraobserver error was <1.5%. Ot.Lc.N/B.Ar per bone area (n/mm^2) were calculated by dividing the total number of lacunae by bone area (excluding nonlacunar porosity). Cell viability within lacunae could not be determined.

In each image, an estimated mean distance between neighboring osteocyte lacunae was also calculated by using the formula shown in figure 2, which allowed for estimates of 2-dimensional and 3-dimensional lacuna-lacuna (Lc-Lc) distances (in microns). This method produced similar values for Lc-Lc distances reported by Weinbaum et al. [1994] who also based these estimations on 2-dimensional Ot.Lc.N/B.Ar data in previous studies.

Spatial heterogeneity of osteocyte lacunae was estimated by calculating the coefficient of variation for each region. This was accomplished by dividing the standard deviation by the mean [Vashishth et al., 2000]. Spatial heterogeneity was examined (1) in the context of strain mode and transcortical region (which correlates with strain magnitude and marrow proximity), and (2) for correlations with On.Ar/T.Ar.

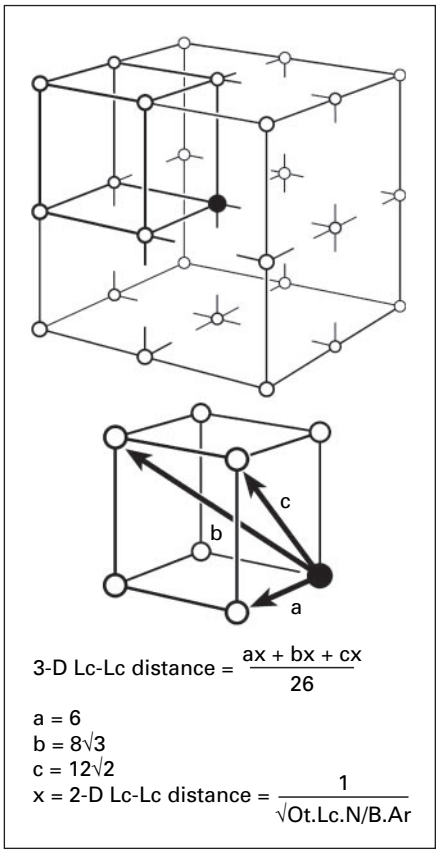

Fig. 2. Three-dimensional (3-D) lattice used to estimate 3-dimensional mean osteocyte Lc-Lc distances from two-dimensional (2-D) Ot.Lc.N/B.Ar data. The equations used for these estimates are also shown.

Additional microstructural and ultrastructural characteristics were also correlated with Ot.Lc.N/B.Ar data. These characteristics, reported in our previous studies using the same images and tissue specimens, included On.N/T.Ar, On.Ar/T.Ar, On.Ar, predominant CFO (see below), porosity, and percent ash. In each bone, cortical thickness measurements were also made at the locations of the images.

In the mid-cortical region of quadrant (radii) or octant (MC3s) locations, predominant CFO was determined using circularly polarized light as previously described [Mason et al., 1995; Skedros et al., 1996]. Regional differences in CFO were quantified in terms of corresponding differences in the transmitted light intensity (expressed as weighted mean gray level), where darker gray levels (lower numerical values) represent relatively more longitudinal CFO, and brighter gray levels (higher numerical values) represent relatively more oblique-to-transverse CFO. The methods used to quantify regional CFO differences in cortical bone as differences in gray

Table 1. Structural and material characteristics by strain mode areas (equine MC3 regions are based on shifting neutral axes shown in figure 1)

Cortical locations	Ot.Lc.N/B.Ar (n/mm^2)	Spatial het	CFO WMGL	On.N/T.Ar n/mm^2	On.Ar/T.Ar %	Ash %	Porosity %	Cort. Th. mm
MC3								
Tension '1' (D, D-L, L)	494.5 (98.8)	0.193	129.1 (20.2)	14.4 (6.5)	36.0 (16.9)	69.5 (5.5)	4.7 (1.6)	9.4 (1.3)
Tension '2' (D-L, L)	474.8 (99.0)	0.207	119.6 (17.4)	13.7 (6.1)	35.3 (16.5)	69.7 (4.8)	4.5 (1.2)	9.3 (1.2)
'C1' (P-L, P, P-M, M, D-M)	463.8 (105.5)	0.207	150.1 (30.0)	16.0 (7.4)	42.7 (16.4)	68.5 (5.9)	5.2 (2.1)	8.4 (1.0)
'C2' (P-L, P, P-M, M)	446.6 (92.6)	0.208	153.7 (28.6)	16.4 (7.1)	43.9 (15.5)	70.8 (7.6)	5.4 (2.3)	7.7 (0.8)
'C3 (P-L, P, P-M)	427.3 (91.8)	0.215	158.5 (26.2)	16.6 (6.6)	44.4 (14.2)	67.0 (5.4)	5.6 (2.6)	6.3 (0.6)
'C4' (P, P-M, M)	451.6 (92.7)	0.206	156.8 (29.7)	16.1 (7.2)	43.1 (15.8)	68.4 (6.3)	5.4 (2.4)	7.9 (0.9)
Radius								
Cr 'tension'	478.2 (137.3)	0.287	89.5 (24.6)	9.4 (5.2)	26.8 (15.2)	68.3 (1.2)	4.4 (2.0)	8.2 (1.0)
Cd 'compression'	522.1 (152.4)	0.291	134.3 (32.7)	18.1 (4.5)	53.7 (12.0)	68.0 (0.8)	4.9 (1.7)	6.7 (0.9)
M	512.7 (129.0)	0.251	82.4 (22.9)	8.5 (4.9)	26.5 (17.4)	68.4 (1.2)	5.2 (1.7)	10.2 (2.0)
L	532.1 (124.9)	0.235	83.6 (29.8)	8.3 (4.1)	24.9 (13.8)	68.8 (1.0)	4.9 (2.5)	8.8 (1.9)

Spatial het = Spatial heterogeneity of osteocyte lacunae; WMGL = weighted mean gray level; Cort. Th. = cortical thickness; C = compression; D = dorsal; D-L = dorsal-lateral; L = lateral; P-L = palmar-lateral; P = palmar; P-M = palmar-medial; M = medial; D-M = dorsal-medial; with the exception of spatial het, the data are shown as means and standard deviations.

levels [Skedros et al., 1996; Bromage et al., 2003] have produced relative differences that are similar to the 'longitudinal structure index' used by others [Martin and Burr, 1989; Martin et al., 1996; Takano et al., 1999; Kalmey and Lovejoy, 2002].

In the MC3s, correlation analyses were also conducted between Ot.Lc.N/B.Ar, the morphologic characteristics, and estimated values of normal and shear strain magnitudes, and summed strain energy densities. Examining normal and absolute values of shear and normal strain also allowed for the assessment of strain mode influences. As described in our previous study [Skedros et al., 1996], these data were obtained from a 2-dimensional finite element model representing the mid-diaphysis of mid-stance loading of Thoroughbred and Quarter horses [Gross et al., 1992].

A multiple comparisons ANOVA model was used for statistical analysis, with 10 and 9 bones for radii and metacarpals, respectively. All possible paired comparisons between cortical *regions* (pericortical, middle cortical and endocortical) and *quadrants* (radii) or *octants* (MC3s) were assessed for statistical significance using a two-way ANOVA (location, region) with Fisher's protected least significant difference post-hoc test (Stat View Version 5.0, SAS Institute Inc., Cary, N.C., USA) [Sokal and Rohlf, 1995]. In the radii, a three-way ANOVA (section, quadrant, intracortical region) was used to determine significance between 50 and 65% section locations. In the equine radii, an alpha level ≤ 0.05 was considered statistically significant. Because of the comparatively large number of comparisons in the MC3s, Bonferroni corrections yielded an alpha level ≤ 0.002 for significance. Comparisons were also made for 'tension' versus 'compression' areas (fig. 1, tables 1, 2). Pearson correlation coefficients were determined for various comparisons, and Spearman correlations were used in the MC3s for strain versus morphologic characteristics.

Table 2. p values for MC3 'tension' versus 'compression' comparisons for Ot.Lc.N/B.Ar and spatial heterogeneity of osteocyte lacunae

	T1	T2	C1	C2	C3	C4
T1		>0.5	>0.5	>0.5	>0.5	>0.5
T2	0.26		>0.5	>0.5	>0.5	>0.5
C1	0.02	0.43		>0.5	>0.5	>0.5
C2	0.001	0.08	0.21		>0.5	>0.5
C3	<0.001	0.006	0.01	0.18		>0.5
C4	0.01	0.17	0.43	>0.5	0.11	

The right upper part represents p values for spatial heterogeneity of osteocyte lacunae, the left lower part the p values for Ot.Lc.N/B.Ar.

'Tension' (T) and 'compression' (C) areas: T1 = D, D-L, L; T2 = D-L, L; C1 = P-L, P, P-M, M, D-M; C2 = P-L, P, P-M, M; C3 = P-L, P, P-M; C4 = P, P-M, M.

D = Dorsal; P = palmar; M = medial; L = lateral.

Results

Equine MC3

In the equine MC3s, comparisons of octant data, i.e. combined region data (pericortical + middle cortical + endocortical within each octant), demonstrated only a few statistically significant differences: (1) 23.5–25.4% higher Ot.Lc.N/B.Ar in the dorsal cortex than in the pal-

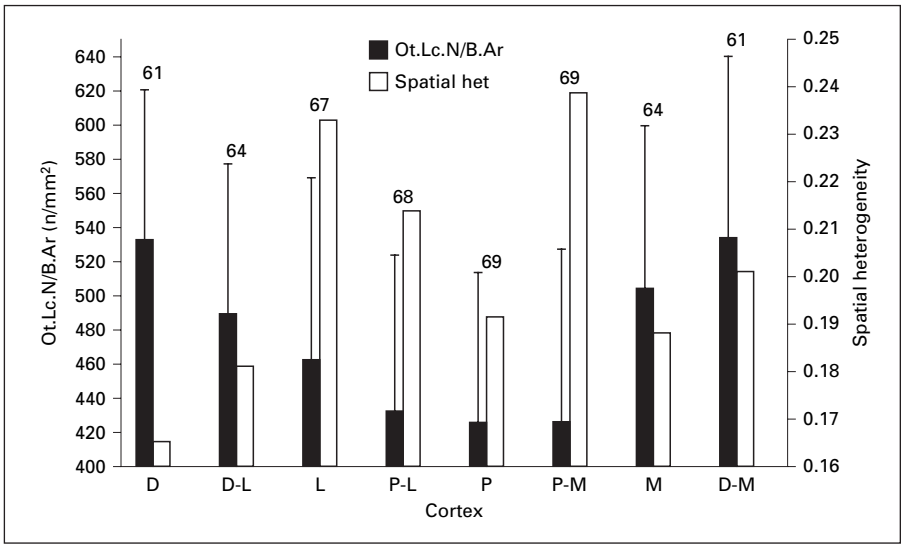

Fig. 3. Equine MC3s: histograms of Ot.Lc.N/B.Ar, estimated Lc-Lc 3-dimensional distances, and spatial heterogeneity (het) of osteocyte lacunae in octant locations. Numbers above bars indicate estimated mean Lc-Lc distance in microns. D = Dorsal; L = lateral; P = palmar; M = medial. The data for Ot.Lc.N/B.Ar are shown as means and standard deviations.

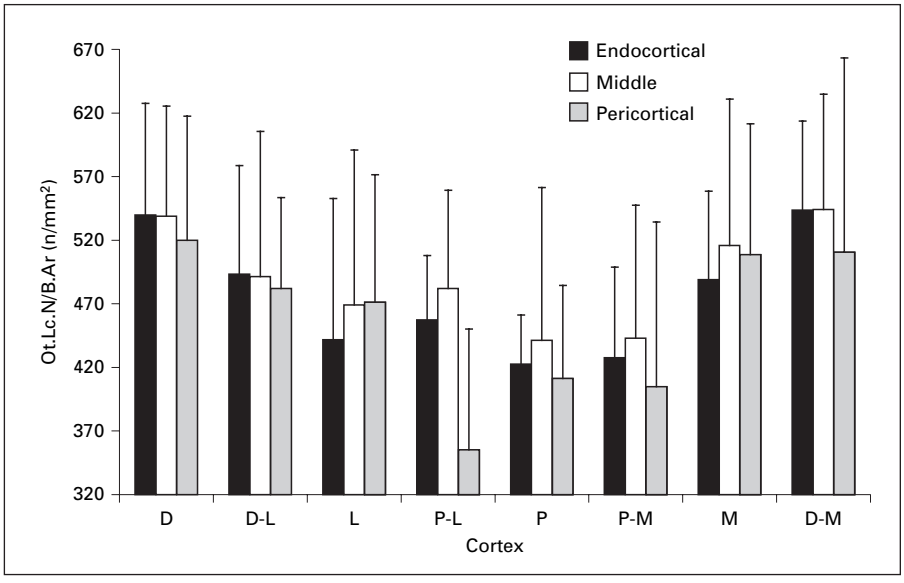

Fig. 4. Equine MC3s: histograms showing Ot.Lc.N/B.Ar in octant 'regions' (pericortical, middle, endocortical). D = Dorsal; L = lateral; P = palmar; M = medial. The data are shown as means and standard deviations.

mar-lateral, palmar and palmar-medial cortices ($p < 0.001$), and (2) approximately 24% higher Ot.Lc.N/B.Ar in the dorsal-medial cortex than in the palmar-lateral, palmar and palmar-medial cortices ($p < 0.001$). These differences, ranging from 425.1/mm^2 to 532.9/mm^2, correspond to a difference in Lc-Lc distance of approximately 8 μm (fig. 3). There were no statistically significant differences (all $p > 0.3$) in coefficients of variation (i.e. estimates of spatial heterogeneity of osteocyte lacunae) in octant comparisons (fig. 3).

Regional comparisons within each octant (i.e. all possible pericortical vs. middle cortical vs. endocortical comparisons at each octant) showed no statistically significant differences (fig. 4). The largest difference shown by these data corresponded to an estimated Lc-Lc distance of approximately 13 μm, reflecting an average Lc-Lc distance range from 62 to 75 μm. Comparisons of spatial heterogeneity using all octant data showed that the endocortical region had generally lower heterogeneity than the middle cortical and endocortical regions ($p = 0.01$ and 0.004, respectively).

In 'tension' area versus 'compression' area comparisons, Ot.Lc.N/B.Ar was on average 8.4% higher (range 2.4–15.8%) in 'tension' than in 'compression' (tables 1, 2). These comparisons were statistically significant in all of the comparisons that used dorsal, dorsal-lateral and

Table 3. MC3 Spearman correlations between strain parameters and morphologic characteristics

	Ot.Lc.N/B.Ar		Spatial het		CFO/WMGL		On.N/T.Ar		On.Ar/T.Ar		Percent ash		Porosity		Cort. Th.	
	r	p	r	p	r	p	r	p	r	p	r	p	r	p	r	p
MC3 Spearman correlations: strain parameters and morphologic characteristics																
Normal strain	0.323	<0.01	–0.086	>0.5	–0.752	<0.01	–0.180	0.01	–0.275	<0.01	0.375	<0.01	–0.119	0.08	0.587	<0.01
Shear strain	0.306	<0.01	–0.019	>0.5	–0.555	<0.01	0.077	0.3	0.062	0.4	–0.277	<0.01	0.010	>0.5	–0.614	<0.01
Peak SED	0.189	0.01	0.031	>0.5	–0.444	<0.01	0.172	0.01	0.284	<0.01	–0.281	<0.01	0.132	0.05	–0.279	<0.01
Summed SED	0.059	0.4	0.146	>0.5	0.579	<0.01	0.116	0.09	0.218	<0.01	–0.108	0.1	0.091	0.19	0.007	>0.5
Correlations of absolute values of normal and shear strains[1]																
Normal strain	–0.345	<0.01	0.065	>0.5	0.166	0.01	0.170	0.01	0.273	<0.01	–0.375	<0.01	0.012	0.08	–0.585	<0.01
Shear strain	0.369	<0.01	0.125	>0.5	–0.287	<0.01	–0.166	0.02	–0.197	<0.01	0.379	<0.01	–0.096	0.16	0.781	<0.01

Spatial het = Spatial heterogeneity of osteocyte lacunae; WMGL = weighted mean gray level; Cort. Th. = cortical thickness; SED = strain energy density.
[1] Absolute values eliminate the influence of the 'sign' of the strain (i.e. where values in compression are negative and values in tension are positive).

lateral locations as the 'tension' area (on average 10.7% higher). In contrast, data in horse radii (see below) show significantly *lower* Ot.Lc.N/B.Ar in the 'tension' area than in the 'compression' area. Only one of the four comparisons was significant when dorsal-lateral and lateral locations were used as the 'tension' area: dorsal-lateral and lateral was 11.1% higher than palmar-lateral, palmar and palmar-medial ($p < 0.01$); otherwise, Ot.Lc.N/B.Ar in the dorsal-lateral and lateral 'tension' area was slightly, but not significantly, higher (approximately 6%) than in the other 'compression' areas ($p \leq 0.08$). In these various comparisons, the differences in corresponding Lc-Lc distances were on the order of 1–5 μm. Lack of significant differences in spatial heterogeneity between 'tension' and 'compression' area comparisons (table 1) also reject the hypothesis that prevalent lamellar osteons in the 'compression' area would be associated with lower spatial heterogeneity.

A previous study of these equine MC3s [Skedros et al., 1996] demonstrated that compared with the palmar-lateral, palmar and palmar-medial 'compression' area, the dorsal, dorsal-lateral and lateral 'tension' area contained an average of 15% higher On.N/T.Ar ($p = 0.04$), 8% higher On.Ar/T.Ar ($p < 0.001$) and 19% greater porosity ($p = 0.04$). In most cortical octants, there are no clear trends in transcortical porosity or On.N/T.Ar. Furthermore, there were no significant regional differences in osteon mean cross-sectional areas and the lateral ('tension') cortex had significantly more longitudinal collagen fibers than the other octant locations: 18.3% higher weighted mean gray level in the palmar-lateral, palmar and palmar-medial 'compression' area versus the dorsal, dorsal-lateral and lateral 'tension' area ($p < 0.001$). The palmar cortices (palmar-lateral, palmar and palmar-medial) were thinner ($p < 0.01$) and had 4% lower percent ash ($p < 0.05$) than the other locations.

Analyses of Ot.Lc.N/B.Ar, spatial heterogeneity of osteocyte lacunae, and each of the structural (i.e. cortical thickness) and material characteristics revealed only two comparisons with a correlation coefficient greater than |0.400|: (1) CFO versus Ot.Lc.N/B.Ar ($r = 0.408$, $p < 0.0001$), and (2) spatial heterogeneity versus On.Ar/T.Ar ($r = 0.511$, $p = 0.01$). The only correlations between material and mechanical parameters that exceeded |0.500| included moderate positive correlations between predominant CFO and normal strain (which considers strain mode) ($r = 0.752$), CFO and shear strain ($r = 0.555$), and CFO and summed strain energy density ($r = 0.579$) (table 3). As shown in table 3, Ot.Lc.N/B.Ar and spatial heterogeneity of osteocyte lacunae exhibited either no, or poor, correlations with the mechanical parameters.

Equine Radius

In the equine radii, a three-way ANOVA showed no statistically significant differences in Ot.Lc.N/B.Ar between the 50 and 65% sections ($p = 0.20$) and among all possible comparisons among the 12 regions ($p = 0.34$). A two-way ANOVA (quadrant, region) demonstrated that bone quadrant (Cr, Cd, medial, lateral) is the only parameter that demonstrated statistically significant differences ($p < 0.05$): (1) 9.2% higher Ot.Lc.N/B.Ar in the Cd 'compression' cortex than in the Cr 'tension' cortex (in the MC3s, the 'compression' area had *lower* Ot.Lc.N/B.Ar than the 'tension' area), and (2) 11.3% higher in the lateral cortex ($p < 0.01$) when compared with the Cr cortex ($p < 0.05$) (fig. 5). The medial cortex had higher Ot.Lc.N/B.Ar than the Cr cortex, but this was a statistical tendency ($p = 0.1$). Although a statistically significant differ-

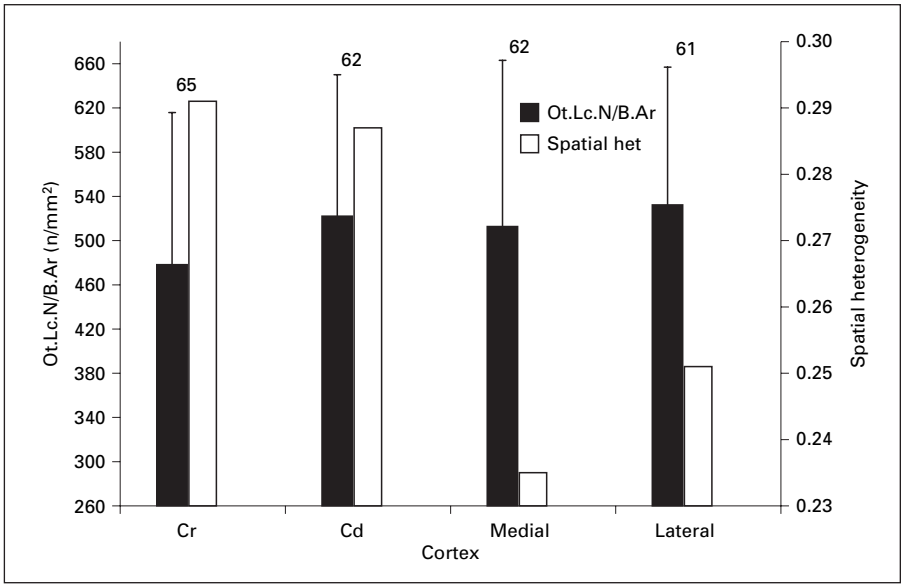

Fig. 5. Equine radii: histograms of Ot.Lc.N/B.Ar, estimated Lc-Lc 3-dimensional distances, and spatial heterogeneity (het) of osteocyte lacunae in quadrant locations. Numbers above bars indicate estimated mean Lc-Lc distance in microns. The data for Ot.Lc.N/B.Ar are shown as means and standard deviations.

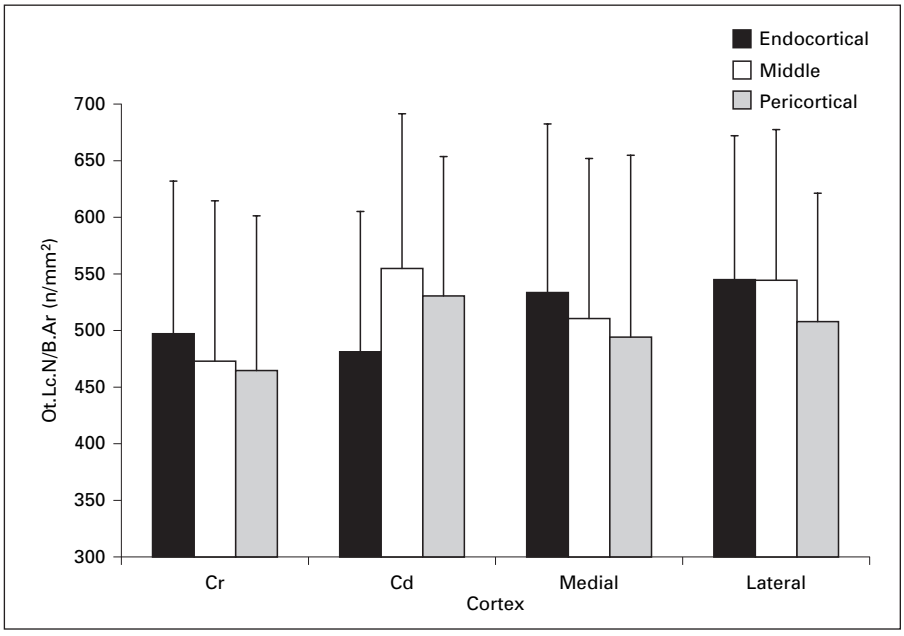

Fig. 6. Equine radii: histograms showing Ot.Lc.N/B.Ar in octant 'regions' (pericortical, middle, endocortical). The data are shown as means and standard deviations.

ence in Lc-Lc distance ($p < 0.0001$) was observed between Cr and Cd cortices, this difference in distances is on the order of 2–3 μm. There were no statistically significant transcortical Ot.Lc.N/B.Ar differences (fig. 6). There were few significant differences in spatial heterogeneity of osteocyte lacunae in quadrants (fig. 5): Cd versus medial ($p < 0.01$), Cr versus lateral ($p = 0.05$), and Cr versus medial ($p < 0.01$).

Our previous study [Mason et al., 1995] showed that the Cd 'compression' cortex of horse radii had 104% higher On.N/T.Ar (8.7/mm^2 vs. 18.1/mm^2; $p < 0.001$) and 108% higher On.Ar/T.Ar (26.0 vs. 56.4%; $p < 0.001$) than the other quadrants. However, data from the present study reject the hypothesis that lamellar osteons in the 'compression' area are associated with lower spatial heterogeneity of osteocyte lacunae than the parallel-fibered osteons in the 'tension' area.

Regional (i.e. transcortical) comparisons within cortical quadrants showed no consistent pericortical-to-endocortical variations in On.N/T.Ar or On.Ar/T.Ar, and os-

teon mean cross-sectional areas were typically slightly larger in the endocortical region than in the middle and pericortical regions. There were no significant porosity differences between the cortical quadrants; however, within each quadrant, the endocortical region was more porous than the middle or pericortical regions. Analysis of predominant CFO showed more oblique-to-transverse fibers in the Cd 'compression' cortex and more longitudinal fibers in the Cr 'tension' cortex ($p < 0.01$), but there were no statistically significant differences between the intracortical regions within these locations, or between the medial and lateral cortices.

There were several statistically significant differences in cortical thickness, but some of these differences were minor (table 1): (1) the Cr cortex was 22.3% thicker than the Cd cortex ($p < 0.01$), (2) the lateral cortex was 31.3% thicker than the Cd cortex ($p < 0.01$), and (3) the medial cortex was 15.9% thicker than the lateral cortex, 52.2% thicker than the Cd cortex and 24.3% thicker than the Cr cortex (all p values <0.001). The percent ash data showed only minor variations (1–2% differences) between the cortical quadrants.

Analyses of Ot.Lc.N/B.Ar or spatial heterogeneity data with cortical thickness, material characteristics and strain parameters showed only two correlation coefficients exceeding |0.500|: (1) spatial heterogeneity versus On.N/T.Ar ($r = 0.590$, $p = 0.04$), and (2) spatial heterogeneity versus On.Ar/T.Ar ($r = 0.539$, $p = 0.07$).

Discussion

Diaphyses of equine MC3s and radii exhibit regional morphologic heterogeneities that appear to be specifically adapted for their non-uniform strain distributions [Boyde and Riggs, 1990; Riggs et al., 1993; Mason et al., 1995; Skedros et al., 1996b; Reilly and Currey, 1999; Batson et al., 2000]. CFO is the characteristic that has been most consistently correlated with the 'tension/compression' distributions in these and other bones that experience habitual bending [Marotti, 1963; Lanyon and Bourn, 1979; Bouvier and Hylander, 1981; Portigliatti Barbos et al., 1984; Riggs et al., 1993; Skedros, 1994a; Skedros et al., 1994b, 1996, 1997; Takano et al., 1999; Skedros, 2001a; Skedros et al., 2001c; Kalmey and Lovejoy, 2002; Skedros et al., 2003b, 2004b]. Correlations of CFO with On.N/T.Ar might reflect osteon-mediated formation of these regional CFO variations. We hypothesized that by being linked with On.N/T.Ar, Ot.Lc.N/B.Ar would also be correlated with CFO. However, this was not the case; only in the MC3 was CFO correlated (weakly, $r = 0.408$) with Ot.Lc.N/B.Ar, and there were no correlations with On.N/T.Ar in either bone. Furthermore, Ot.Lc.N/B.Ar inconsistently/poorly correlated with local strain-related characteristics (including strain magnitude and mode) and structural/material heterogeneity (including On.Ar and cortical thickness). As discussed below, approximations of regional Lc-Lc distances suggest that even in the few instances where statistically significant differences in Ot.Lc.N/B.Ar and/or the spatial heterogeneity of lacunae were observed, these variations are not biomechanically significant. Our data are also considered in the context of literature reviews of osteocyte intercellular communication, microdamage detection and metabolism/nutrition requirements.

This study has several possible limitations. We were unable to determine osteocyte viability, which could confound some of our interpretations, especially if there are significant regional differences in cell viability. For example, Power et al. [2001] reported 50–70% lacunar occupancy in cortical bone from femoral neck cortices of elderly human females. These data are consistent with earlier studies showing that the percentage of empty lacunae increases with age in human bones [Frost, 1960; Baud and Auil, 1971; Wong et al., 1985; Wong et al. 1987; Mullender et al. 1996a, 1996b]. Consequently, the age-related decline in osteocyte density is probably more pronounced than the age-related decline in lacuna density [Vashishth et al., 2000]. However, our specimens were from relatively young adults, and our observations did not reveal regions with lacunae that were plugged with hypermineralized tissue, which has been associated with aging, ischemia or necrosis [Frost, 1960; Currey, 1964; Kornblum and Kelly, 1964; Jowsey, 1966; Stout and Simmons, 1979; Parfitt, 1993a]. These observations and the estimated 'younger' ages of our animals suggest that the percentage of dead osteocytes is small; this is consistent with observations of >90% lacuna occupancy in the dorsal cortex of MC3s from Thoroughbred and Quarter horses similar in age to those used in the present study [Gómez et al., 2005; P. Muir, pers. commun.].

Regional Cell-Cell or Cell-Matrix Adaptations without Remodeling or Modeling

Similar to Marotti et al. [1990], Marotti [1996, 2000] and Metz et al. [2003], other investigators have considered the possibility that osteocytes form a repressive network that downregulates bone remodeling [Noble and Reeve, 2000; Heino et al., 2002; Power et al., 2002; Qiu et al., 2002b]. Data in the present study suggest that the osteocytic repression of resorption, and other mechano-

sensory functions attributed to osteocytes, if present and if significantly different between the locations examined, are not accomplished with regional adjustments in their densities. This conclusion seems to be supported by a study by Robling and Turner [2002] who examined Ot.Lc.N/B.Ar in three inbred strains of mice with significant differences in mechanosensitivity. Two strains of mice had significantly different Ot.Lc.N/B.Ar but nearly identical mechanosensitivity, and a third strain with similar Ot.Lc.N/B.Ar to one of these other strains had lower mechanosensitivity. They concluded that osteocyte densities are not correlated with mechanosensitivity. In contrast, in a study correlating Ot.Lc.N/B.Ar with age-related microdamage prevalence in human femoral diaphyses, Vashishth et al. [2000] suggested that mechanosensitivity and Ot.Lc.N/B.Ar *are* correlated.

These conflicting conclusions can be reconciled by the possibility that a habitual strain milieu, even if highly non-uniform, might *not* be sufficient for requiring regional adjustments in Ot.Lc.N/B.Ar as a means for modifying the 'sensitivity' of the osteocyte mechanosensory network. It has been suggested that regional cell-cell or cell-matrix accommodations for the ambient strain milieu might be achieved without evoking remodeling/modeling or changing osteocyte densities [Pavalko et al., 1998; Rubin et al., 2002]. For example, Rubin et al. [2002, p. 264] state that '… the osteocyte is capable of "normalizing" [sic] its local mechanical environment by modulating its cytoskeletal architecture, attachment to the matrix, configuration of the periosteocytic space, and communication channels to surrounding cells'. Other forms of 'communication' such as paracrine signaling or canaliculi fluid pressure generation in the contiguous lacunocanalicular fluid space might be employed in establishing communicating cellular networks rather than by direct intercellular responses of osteocytes to mechanical stresses [Knothe Tate, 2003]. But even these are likely linked to tissue deformation [Weinbaum et al., 1994, 2001; Ehrlich et al., 2002]. Additionally, as suggested by Srinivasan and Gross [2000], it is possible that regional variations in load-related fluid flow dynamics can have important effects on osteocyte physiology, which further confounds interpretations linking osteocyte densities to local biomechanics. In view of these possibilities, it is suggested that either (1) the heterogeneous material organization and relatively uniform osteocyte densities of the equine radii and MC3s reflect the achievement of tissue organizations that are adequate for both cell-matrix and cell-cell interactions, or (2) the cell densities are *not* adequate for mechanobiological functions; hence, regional cell level 'adaptations' are present.

Social/Communication Functions: Wiring Transmission versus Volume Transmission

Marotti [2000] has suggested that intercellular communication between osteocytes can occur via 'wiring transmission', similar to interneuronal signals. Turner et al. [2002] suggest that, analogous to neuronal systems, communicating cellular networks in bone (i.e. osteocytes, osteoblasts and bone-lining cells) exhibit basic properties of short- and long-term memory. Such cellular communication could be responsible for the different adaptations or sensitivities to mechanical stress observed between different bones of the same animal and between different parts of the same bone. This may occur via desensitization mechanisms that dampen communication between cells subjected to repetitive mechanical loading. Conversely, bone cell populations could become sensitized to signals by mechanisms similar to those that cause neuronal sensitization. In view of our results, these 'neurologic' capacities, even if present, are probably not influenced by regional variations in osteocyte density.

In contrast to wiring transmission, 'volume transmission' (which is not dependent on osteocytic intercellular communication) is more strongly influenced by paracrine/autocrine stimulation [Marotti, 2000; Palumbo et al., 2004]. Consequently, hypothesized osteocytic 'volume/population' responses are not necessarily dependent on cell density and are probably not significantly perturbed by microdamage [Tami et al., 2002]. For example, volume transmission may explain osteocyte responses in experimental and normal loading of adult rat ulnae in studies measuring the presence of estrogen receptor-α in osteocytes [Ehrlich et al., 2002]. The distribution of cells expressing estrogen receptor-α was uniform across all sections – not reflecting the non-uniform local peak strain magnitudes. They suggest that because '… osteocytes appeared to respond in concert to the strain-related stimulus this suggests that they communicate and act together as a population, rather than as individual strain-responsive cells'. However, an important role for wiring transmission cannot be precluded. Donahue [2000] also notes that since only a small percentage (approximately 30%) of osteoblastic cells in a cell ensemble respond to hormones or growth factors (e.g., parathyroid hormone), on an individual basis, they can communicate this response to other cells via gap junctions such that the ensemble response is greater than the sum of the response of individual cells. Additional studies are needed to determine the relative importance of 'wiring transmission' and 'volume transmission'.

Osteocytic 'Operational' Networks for Microdamage Detection: Associations with Strain Mode and Strain Gradients

The possibility that osteocyte lacunae may be stress concentrators for microdamage formation has long been speculated, and this relationship may increase with age or excessive exercise [Currey, 1962; Prendergast and Huiskes, 1995; McCreadie and Hollister, 1997; Nicolella et al., 1997; Reilly, 2000; Kim et al., 2004]. For example, Reilly's [2000] confocal microscopic observations of tangential beams of diaphyseal cortices of bovine, equine and human limb bones loaded in tension and bending showed that microdamage appears to initiate at, or in close association with, osteocyte lacunae. However, Reilly [2000, p. 1131] noted that in '… previous microdamage investigations only compression cracking has been shown to be influenced by [osteocyte] lacunae [Carter and Hayes, 1976]'. Thus, habitual compression environments may be where modifications in Ot.Lc.N/B.Ar are most beneficial. In view of these observations, we hypothesized that Ot.Lc.N/B.Ar in equine radii and MC3s would exhibit strain mode/magnitude differences between their 'tension', 'compression' and 'shear' (neutral axis) cortices. In turn, it seemed plausible that osteocyte densities could differ between regions habitually exposed to different strain modes, reflecting 'sensor' densities required for monitoring corresponding differences in microdamage formation. This speculation was based on a study of human femoral diaphyses (mean age approximately 43 years) where Vashishth et al. [2000] proposed that a minimum number of osteocytes are required for an 'operational' network that detects, and hence prevents, large increases in microcrack density. This is also consistent with the idea that osteocytes play an important role in the targeted detection of microdamage [Martin, 2000; Verborgt et al., 2000; Tami et al., 2002; Martin, 2003; Qiu et al., 2005].

These hypotheses are indirectly supported by studies showing that microdamage incidence and/or morphology in fatigue-loaded bone are highly correlated with strain magnitude and mode. For example, in strain-mode-specific loading (e.g., compression testing of bone from a habitually compression-loaded region), Reilly [2000] examined in vivo-loaded rat ulnae that were loaded high enough to cause permanent deformation. En bloc fluorescein staining and confocal microscopy revealed diffuse damage composed of arrays of tiny (<10 μm) microcracks in the lateral cortex, which was loaded in tension (its habitual loading mode). Reilly and Currey [1999] mechanically tested tangential beam specimens from Cr ('tension') and Cd ('compression') cortices of a radius of an 11-year-old Thoroughbred. All specimens were loaded in four-point bending. En bloc fluorescein staining and confocal microscopy showed that (1) tension microcracks first appeared at a strain of approximately 0.004 compared to compression at 0.008–0.010, (2) specimens from the Cd 'compression' cortex showed little compression microcracking, and such microcracks were small and diffuse (these specimens first failed in tension on the tension side of the beam), and (3) specimens from the Cr 'tension' cortex showed comparatively more numerous compression microcracks, which were longer and less diffuse (these specimens initially failed in compression on the compression side of the beam). Typically, compression microcracks were tiny, on the order of 5 μm. However, unlike tension microcracks, which seemed to be limited to tens of microns, many compression microcracks were very long, on the order of several hundred microns. Reilly and Currey [1999, p 551] concluded that:

> … Bone can be adapted to be better at resisting the growth of one type of microcrack (either tension or compression) but that this then causes it to be bad at resisting the other type. Therefore, it is better for bone to be loaded in one mode only, so that it can adapt histologically to that mode.

In view of these findings, we hypothesized that a consistent tension/compression/shear distribution across a bone cross-section may, by introducing regional strain magnitude/mode-related microdamage, ultimately contribute to regional differences in remodeling-mediated heterogeneity (e.g., On.N/T.Ar, osteon orientation, predominant CFO) that occurs during the ontogenetic development of equine MC3s and radii, and other limb bones [Stover et al., 1992; Riggs et al., 1993; Skedros and Kuo, 1999; Skedros et al., 2002; Skedros and Hunt, 2004a; Skedros et al., 2004b]. In turn, we speculated that regional variations in Ot.Lc.N/B.Ar would be linked with these 'histologic adaptations'. However, the MC3s and radii exhibited opposite Ot.Lc.N/B.Ar differences in 'tension' versus 'compression' comparisons. As discussed in a companion study of regional Ot.Lc.N/B.Ar variations in artiodactyl and perissodactyl calcanei [Skedros, 2005], this difference may represent 'adaptations' in the relatively simple bending environment of the radius that are obscured by tissue adaptations of the more complex torsion/bending environment of the MC3.

It is also possible that normal maturation-related remodeling progressively curbs the occurrence of microdamage, reducing the hypothesized regional variations in Ot.Lc.N/B.Ar. Remodeling can restrict further microdamage formation, growth or accumulation by introducing in-

terfaces and improving the matrix in other ways (e.g., CFO realignment, osteocyte repopulation and/or adjusting relative percentages of osteon morphotypes), which can modify microdamage initiation, propagation and arrest [Martin et al., 1998; Hiller et al., 2003]. This process has been described as progressive 'toughening', and there are data supporting the suggestion that this normally occurs during skeletal ontogeny [Reilly et al., 1997; Skedros et al., 2004b; Sobelman et al., 2004; Nalla et al., 2005].

Preferential resorption of bone, and repopulation of cortical osteocytes, may produce the clustering of osteocytes, which can increase their spatial heterogeneity [Vashishth et al., 2000]. In femoral neck cortices of elderly human females (mean age 82.2 ± 3 years), Power et al. [2002] have also shown higher Ot.Lc.N/B.Ar in resorbing and forming osteons compared with quiescent osteons. If this relationship is typical of cortical remodeling, then the elimination of microdamage would produce regions with relatively lower Ot.Lc.N/B.Ar. This possibility might be reflected by our data showing moderate positive correlations between On.Ar/T.Ar and spatial heterogeneity of osteocyte lacunae (MC3s: $r = 0.511$, $p = 0.01$; radii: $r = 0.539$, $p = 0.07$). Consequently, even if Ot.Lc.N/B.Ar initially correlated with a prevalent/predominant strain mode/magnitude in these bones, remodeling-mediated osteocytic repopulation of the cortex may obscure such associations.

An important point to consider here is that neither strain mode nor strain magnitude may be driving forces behind the organization and distribution of osteocytes within the bone matrix, and that other biomechanical factors may be involved. Specifically, it has been hypothesized that strain gradients regulate the osteogenic response to increased loading that accompanies increased physical activity [Gross et al., 1997; Judex et al., 1997b]. As noted earlier, changes in fluid flow within the lacunocanalicular system of bone regulate not only osteocyte viability but also the osteogenic signals generated by osteocytes (fig. 7). Strain gradients generate pressure differentials within bone, and these pressure differentials increase fluid movement within the lacunocanalicular network [Gross et al., 1997]. If the percentage of osteoblasts that differentiate to form osteocytes is held constant, then osteocyte density should be proportional to the bone formation rate. Experimental data indicate that activation of mineralizing bone surfaces is correlated with strain gradients [Judex et al., 1997b; Srinivasan and Gross, 2000], which suggests that areas of high strain gradients would also be associated with increased bone formation rates and hence osteocyte densities. Areas with high circumferential strain gradients often do not correspond to areas of peak strain, and in fact, peak strain gradients are frequently located nearest the neutral axis of bending [Judex et al., 1997]. It is worth noting here that in the case of the equine MC3, the highest values for Ot.Lc.N/B.Ar are in the dorsal, dorsal-medial and dorsal-lateral regions, which also happen to be closest to the neutral axes (fig. 1, 3). Likewise, the highest values for Ot.Lc.N/B.Ar in the equine radius are in the lateral region, also closest to the neutral axes. Clearly, additional data on strain gradients within the cortices of the equine MC3 and radius are needed to confirm these hypotheses; however, the data presented herein indicate that although Ot.Lc.N/B.Ar does not always track specific patterns of strain-mode-specific loading, osteocyte densities may correspond to areas of high circumferential strain gradients.

Mechanical Influences of Ot.Lc.N/B.Ar

Results of an analytical study [Yeni et al., 2001] suggest that Ot.Lc.N/B.Ar can significantly influence the apparent stiffness of the bone matrix ('matrix' refers to hard tissue containing lacunae without microstructural pores such as central canals); however, the differences were small within the physiologic Ot.Lc.N/B.Ar range. Our recent ex vivo mechanical testing studies of mature equine MC3 diaphyses show that Ot.Lc.N/B.Ar can have important influences on bone mechanical properties in strain-mode-specific testing [Skedros et al., 2001b, 2003c; unpubl. data]. For example, in strain-mode-specific compression tests, Ot.Lc.N/B.Ar was, among several characteristics (percent ash, porosity, mean osteon cross-sectional areas, On.N/T.Ar and CFO), the first or second most important in explaining observed variation in stiffness (Young's elastic modulus), yield and ultimate stress, as well as pre-yield (elastic) energy absorption. In strain-mode-specific testing of dorsal ('compression') cortices of mule deer calcanei, Ot.Lc.N/B.Ar was the third most important histocompositional characteristic in explaining variance in these three mechanical parameters [Skedros et al., 2003b; unpubl. data). Additionally, in these deer calcanei and equine MC3s, the correlations of Ot.Lc.N/B.Ar with stiffness, yield and ultimate stress, and elastic energy were *negative*, suggesting that osteocyte lacunae may have a significant role as stress concentrators in these ex vivo compression tests. Fatigue testing and more rigorous fracture toughness testing may reveal additional important and more physiologically relevant roles for Ot.Lc.N/B.Ar in the mechanical behavior of cortical bone.

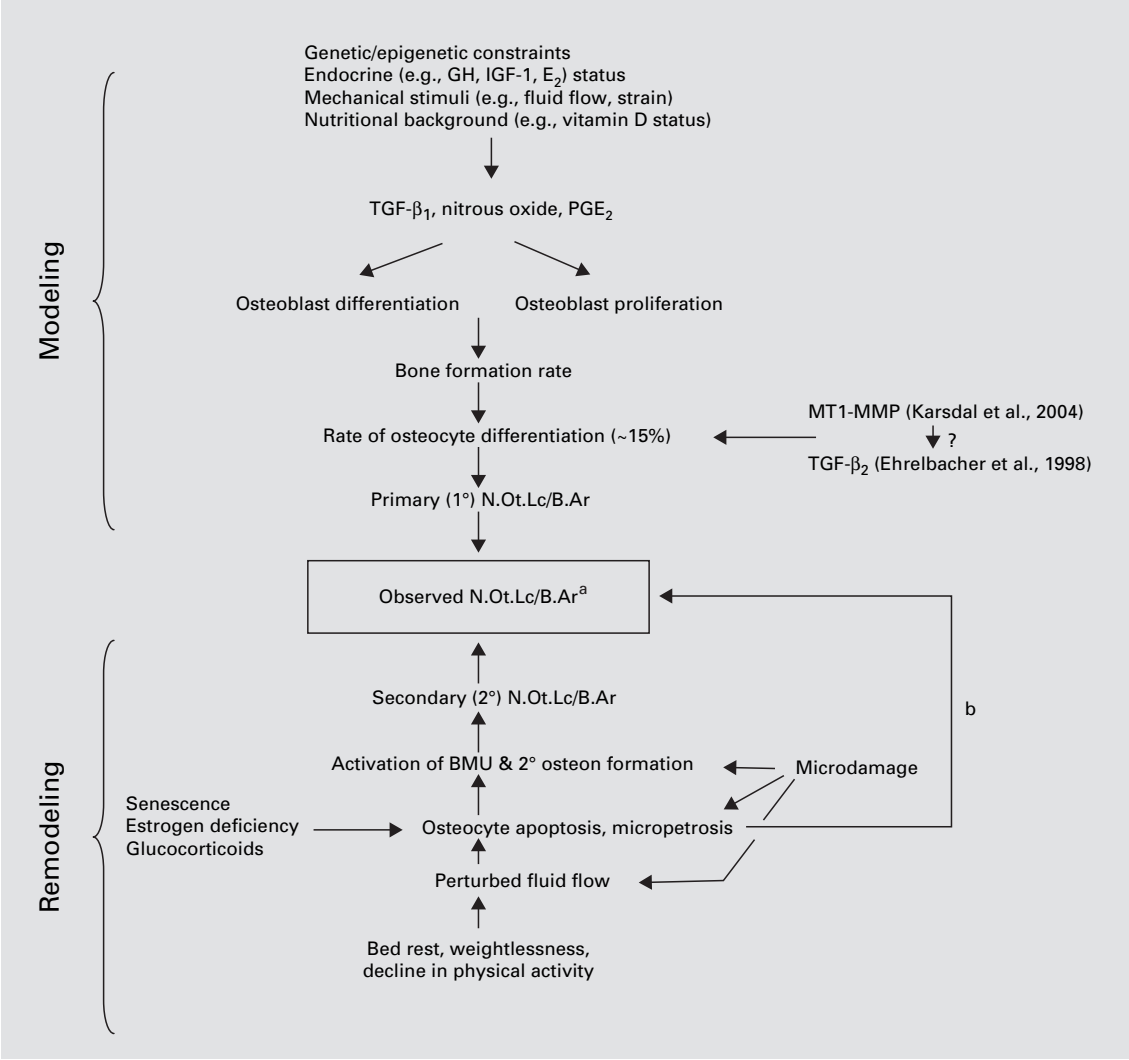

Fig. 7. Diagrammatic representation of modeling and remodeling and related influences on osteocyte densities in cortical bone. GH = Growth hormone; IGF-1 = insulin-like growth factor 1; E_2 = estradiol; TGF-β_1 = transforming growth factor-β_1; PGE_2 = prostaglandin E_2; MT1-MMP = membrane type 1 matrix metalloproteinase; BMU = basic multicellular unit. [a] Cortical bone; [b] osteocytes and osteocyte lacuna numbers can be affected independent of modeling/remodeling.

Metabolic Rate and Species- or Tissue-Specific Requirements of Ot.Lc.N/B.Ar

Osteocyte density may be directly proportional to metabolic rate, i.e. animals with a higher metabolism, and hence in greater need for immediate mineral access, would have higher osteocyte densities [Mullender et al., 1996a; Cullinane, 2002]. In this context, we speculated that endocortical regions showing increased remodeling activity would exhibit relatively higher Ot.Lc.N/B.Ar. Mullender et al. [1996a], reporting data generally supporting this idea, compared osteocyte densities in *trabecular* bone of femoral heads of adult animals of five different species (rat, rabbit, monkey, pig, cow) and found that osteocyte density negatively correlated with body size. They suggest that the metabolic rate might be an important determinant of osteocyte density since body size is negatively correlated with the basal metabolic rate. However, Remaggi et al. [1998] did not find a similar relationship in *cortical* bone of mature limb bone diaphyses of various species. They examined tibiae in humans and dogs (n = 3 each), femora in frogs, chicks, and rabbits (n = 3 each), and MC3s in horses and cows (n = 3 each) [F. Remaggi, pers.

commun.] (table 4). Ferretti et al. [1999] corroborated these findings in a study examining lamellar osteons and parallel-fibered osteons in the cortices of mature limb bones of frogs, sheep, dogs, cows, horses and humans. They suggested that bone histology, not animal size or metabolic rate, is relatively more important in producing species variations in Ot.Lc.N/B.Ar, and noted that this is '… in sharp contrast with Mullender's view [Mullender et al., 1996a], according to which a positive correlation would seem to exist between osteocyte volume and animal body size' [Feretti et al., 1999, pp. 129–130].

Ferretti et al. [1999] also showed that Ot.Lc.N/B.Ar was higher in woven bone, intermediate in parallel-fibered secondary osteons, and lower in lamellar secondary osteons, reflecting the more 'orderly' cell recruitment and more regular matrix of lamellar osteons. Since in mammals woven bone is typically found in early skeletal development or in rapid bone formation, osteocyte densities in this tissue might reflect growth-related nutritional/metabolic demands. Woven bone is a component of the fibrolamellar histology (a type of primary bone) common in the appendicular skeletons of some large mammals, including deer, cows and horses (including the primary bone in our specimens) [Stover et al., 1992; Currey, 2002; Mori et al., 2003; Skedros et al., 2003c]. Although our data showed that Ot.Lc.N/B.Ar and On.Ar/T.Ar were poorly correlated, it is possible that the histology of our specimens was not sufficiently variable to rigorously test the hypothesis that Ot.Lc.N/B.Ar is relatively higher in primary bone.

If osteocytes have an important role in mineral acquisition, then significant mineral mobilization can occur across quiescent lacunocanalicular surfaces [Aarden et al., 1994; Cullinane, 2002; Martin, 2003; Parfitt, 2003]. Three main mechanisms exist by which calcium (Ca) exchange can occur across quiescent surfaces and beneath bone-lining cells [Heaney, 2003; Parfitt, 2003]: (1) osteocytic osteolysis, which was once thought to be important for Ca exchange and probably occurs in some situations [Aarden et al., 1994; Rodionova et al., 2002; Tazawa et al., 2004], in most cases has a minor role compared with isoionic and heterionic exchange [Heaney, 2003]; (2) isoionic exchange of bone Ca for extracellular Ca, which may be the most significant exchange mechanism, but does not significantly change extracellular Ca levels, and (3) heterionic exchange of bone Ca for extracellular carbonate, which, in contrast to (1) and (2), is an important short-term buffer for Ca concentration. All areas in bone with microvascularization (e.g., Haversian canals, primary vascular canals) can exchange Ca for carbonate only to a depth of approximately 10 microns [Parfitt, 2003]. Parfitt [2003] suggests that since this depth decreases with aging, bone must periodically remodel to keep bone sufficiently young for efficient buffer function. Hence, stochastic remodeling (i.e. not 'targeted' for repairing microdamage) and buffering may be linked in this context, and this may represent a link between Ot.Lc.N/B.Ar, metabolism and remodeling. However, several investigators have favored the hypothesis that bone-lining cells, not osteocytes, manipulate Ca solubility [Parfitt, 1987; Staub et al., 1989; Parfitt, 1993b; Talmage et al., 2000; Qiu et al., 2002a] on inactive surfaces in response to Ca-regulating hormones. Nevertheless, mechanisms for mobilizing Ca across quiescent surfaces are probably only important for short-term Ca mobilization (e.g., on the scale of hours, such as between meals) and not for high demand or long-term needs that require bone remodeling to mobilize relatively large amounts of Ca [Bowman and Miller, 2001; Heaney, 2003]. Therefore, the remodeling process appears to be the major means for accessing Ca in bone, and osteocytes probably do not play a pivotal role in mineral homeostasis.

Scaling Effects of Fatigue Strength and Bone Robusticity on Ot.Lc.N/B.Ar and Histologic Variations

Larger structures are more prone to failure than small structures. An explanation for this difference is that failures are initiated at flaws in the material of a structure, and larger volumes are more likely to contain a significant flaw [Martin, 2003]. Taylor [2000], applying this to bone, argues that large structures are more prone to fatigue failure than smaller structures made of the same material. This implies that bones in larger animals cannot withstand as much stress in daily use as bones in smaller animals. Hence, a bone from a large animal would be comparatively weaker, with the stress concentrator effect of lacunae also contributing disproportionately. Taylor [2000] suggests that this paradox is resolved by 'enhancing' bone material in larger animals. Fatigue-related requirements are therefore important for understanding the biomechanical bases for variations in Ot.Lc.N/B.Ar and other histomorphologic characteristics between different 'stressed volumes' of bones of small and large animals. This interpretation may help to explain such differences within/between bones of the same limb (e.g., between thin/thick cortices or gracile/robust bones) [Skedros et al., 2003a, 2004b]. However, our results in equine radii showing minor Cr-Cd cortical thickness differences suggest that differences in 'stressed volumes' cannot account per se for their histological differences. Consequently, it is not clear if Taylor's explanation works for different 'volumes' within the same cross-section of a bone. Stud-

Table 4. Osteocyte and Ot.Lc.N/B.Ar literature review

Species	Age	Bone	Cortical/ cancellous	Histology	Location	Section thick-ness µm	Method/ stain	Ot.Lc.N/ B.Ar n/mm^2	2-D Lc-Lc distance µm	3-D Lc-Lc distance µm	Percent occu-pancy	Cells or lacu-nae	Reference
Homo sapiens	fetal	mandible	cortical	1°	unk	40–200	l.m.	825	35	49	unk	l	Hobdell
Homo sapiens	adult	mandible	cortical	2°	unk	40–200	l.m.	550	43	60	unk	l	and Howe
Rattus rattus	young	mandible	cortical	1°	unk	40–200	l.m.	1,025	31	44	unk	l	[1971]
Rattus rattus	old	mandible	cortical	1°	unk	40–200	l.m.	850	34	49	unk	l	
Loxodonta africana	fetal	mandible	cortical	1°	unk	40–200	l.m.	850	34	49	unk	l	
Trichechus manatus	fetal	mandible	cortical	1°	unk	40–200	l.m.	1,000	32	45	unk	l	
Canis familaris	fetal	mandible	cortical	1°	unk	40–200	l.m.	1,000	32	45	unk	l	
Manis temmincki	fetal	mandible	cortical	2°	unk	40–200	l.m.	575	42	59	unk	l	
Calotes sp.	fetal	long bones	cortical	1°	diaphyses	40–200	l.m.	1,350	27	39	unk	l	
Lacertidae	fetal	long bones	cortical	1°	diaphyses	40–200	l.m.	1,225	29	40	unk	l	
Iguana iguana	fetal	long bones	cortical	1°	diaphyses	40–200	l.m.	1,225	29	40	unk	l	
Agama stellio	fetal	long bones	cortical	1°	diaphyses	40–200	l.m.	975	32	45	unk	l	
S. stenodactylus	fetal	long bones	cortical	1°	diaphyses	40–200	l.m.	1,000	32	45	unk	l	
Varanus sp.	fetal	long bones	cortical	1°	diaphyses	40–200	l.m.	1,600	25	35	unk	l	
Varanus niloticus	fetal	long bones	cortical	1°	diaphyses	40–200	l.m.	1,050	31	44	unk	l	
Anolis	fetal	long bones	cortical	1°	diaphyses	40–200	l.m.	1,225	29	40	unk	l	
Caimen sclerops	fetal	long bones	cortical	1°	diaphyses	40–200	l.m.	975	32	45	unk	l	
Lissemys punctata	fetal	long bones	cortical	1°	diaphyses	40–200	l.m.	1,650	25	35	unk	l	
Gopherus berlandieri	fetal	long bones	cortical	1°	diaphyses	40–200	l.m.	1,175	29	41	unk	l	
Testudo pardalis	fetal	long bones	cortical	1°	diaphyses	40–200	l.m.	1,350	27	39	unk	l	
Terapene carolina	adult	long bones	cortical	2°	diaphyses	40–200	l.m.	800	35	50	unk	l	
Pythonidae	fetal	long bones	cortical	1°	diaphyses	40–200	l.m.	1,350	27	39	unk	l	
Sphenodon	adult	long bones	cortical	2°	diaphyses	40–200	l.m.	775	36	51	unk	l	
Data were tabulated in orders and families only													
Rodentia	immature	rib, tib, fem	cortical	1°	mid-diap	10	l.m./h&e	113	94	133	>96	c, l	Singh et al.
Marsupialia	unk	rib, tib, fem	cortical	1°	mid-diap	10	l.m./h&e	122	91	128	>96	c, l	[1974]
Insectivora	unk	rib, tib, fem	cortical	1°	mid-diap	10	l.m./h&e	150	82	116	>96	c, l	
Artiodactyla	mature	rib, tib, fem	cortical	1°	mid-diap	10	l.m./h&e	193	72	102	~85	c, l	
Carnivora													
Felidae	immature	rib, tib, fem	cortical	1°	mid-diap	10	l.m./h&e	252	63	89	~78	c, l	
Canidae	aged	rib, tib, fem	cortical	1°	mid-diap	10	l.m./h&e	235	65	92	~72	c, l	
Mustelidae	aged	rib, tib, fem	cortical	1°	mid-diap	10	l.m./h&e	160	79	112	~95	c, l	
Primate													
Pongidae	adult	rib, tib, fem	cortical	1°	mid-diap	10	l.m./h&e	102	99	140	~90	c, l	
Ceropithecidae	newborn	rib, tib, fem	cortical	1° and 2°	mid-diap	10	l.m./h&e	200	71	100	~97	c, l	
Lemuridae	mature	rib, tib, fem	cortical	1°	mid-diap	10	l.m./h&e	212	69	97	>98	c, l	
Cebidae	immature	rib, tib, fem	cortical	1° and 2°	mid-diap	10	l.m./h&e	182	74	105	~78	c, l	
Hominidae	40–60 yrs	rib, tib, fem	cortical	1°	mid-diap	10	l.m./h&e	250	63	90	~68	c, l	
Dog	18, 24, 32 mo	femur	cortical	2°	mid-diap	20–30	l.m.	301	61	86	unk	l	Canè et al.
	18, 24, 32 mo	tibia	cortical	2°	mid-diap	20–30	l.m.	320	51	72	unk	l	[1982]
	18, 24, 32 mo	humerus	cortical	2°	mid-diap	20–30	l.m.	363	52	74	unk	l	
Frog	unk	unk limb	cortical	1°	mid-diap	30–40	l.m.	1,200	29	41	unk	l	Marotti.
Frog	unk	unk limb	cortical	1°	mid-diap	30–40	l.m.	1,290	28	39	unk	l	et al.
Tortoise	unk	unk limb	cortical	1°	mid-diap	30–40	l.m.	1,100	30	43	unk	l	[1990]
Tortoise	unk	unk limb	cortical	1°	mid-diap	30–40	l.m.	2,350	21	29	unk	l	
Chicken	unk	unk limb	cortical	1°	mid-diap	30–40	l.m.	1,875	23	33	unk	l	
Chicken	unk	unk limb	cortical	1°	mid-diap	30–40	l.m.	2,100	22	31	unk	l	
Rat	unk	unk limb	cortical	1°	mid-diap	30–40	l.m.	925	33	47	unk	l	
Rat	unk	unk limb	cortical	1°	mid-diap	30–40	l.m.	2,850	19	27	unk	l	
Rabbit	unk	unk limb	cortical	1° and 2°	mid-diap	30–40	l.m.	900	33	47	unk	l	
Rabbit	unk	unk limb	cortical	1° and 2°	mid-diap	30–40	l.m.	1,925	23	32	unk	l	
Bovine	unk	unk limb	cortical	2°	mid-diap	30–40	l.m.	650	39	56	unk	l	
Bovine	unk	unk limb	cortical	2°	mid-diap	30–40	l.m.	1,850	23	33	unk	l	
Horse	unk	unk limb	cortical	2°	mid-diap	30–40	l.m.	1,025	31	44	unk	l	
Horse	unk	unk limb	cortical	2°	mid-diap	30–40	l.m.	1,700	24	34	unk	l	
Dog	unk	unk limb	cortical	2°	mid-diap	30–40	l.m.	350	53	76	unk	l	
Dog	unk	unk limb	cortical	2°	mid-diap	30–40	l.m.	2,100	22	31	unk	l	
Human	unk	unk limb	cortical	2°	mid-diap	30–40	l.m.	525	44	62	unk	l	
Human	unk	unk limb	cortical	2°	mid-diap	30–40	l.m.	1,050	31	44	unk	l	

Table 4 (continued)

Species	Age	Bone	Cortical/ cancellous	Histology	Location	Section thick-ness µm	Method/ stain	Ot.Lc.N/ B.Ar n/mm^2	2-D Lc-Lc distance µm	3-D Lc-Lc distance µm	Percent occu-pancy	Cells or lacu-nae	Reference
Dolphin	unk	unk limb	cortical	2°	mid-diap	30–40	l.m.	875	34	48	unk	l	
Dolphin	unk	unk limb	cortical	2°	mid-diap	30–40	l.m.	1,400	34	48	unk		
This value, used in a computational analysis, was estimated (methods not stated) from Canè et al. [1982] and Marotti et al. [1990]										35			Weinbaum et al. [1994]
Wistar rat	7 mo	femur	cancellous	–	head	20–40	l.m./h&e	943	33	46	unk	c	Mullender
Rabbit	1.5 yrs	femur	cancellous	–	head	20–40	l.m./h&e	679	38	54	unk	c	et al. [1996a]
Rhesus monkey	4.5–6.7 yrs	femur	cancellous	–	head	20–40	l.m./h&e	400	50	71	unk	c	
Domestic pig	2.6–3.4 yrs	femur	cancellous	–	head	20–40	l.m./h&e	400	50	71	unk	c	
Domestic bovine	3.2–9.6 yrs	femur	cancellous	–	head	20–40	l.m./h&e	295	58	82	unk	c	
Human controls	<55 yrs	ilium	cancellous	–		5	l.m./Gol	207	70	99	84	l	Mullender
	>55 yrs	ilium	cancellous	–		5	l.m./Gol	166	78	110	81	l	et al. [1996b]
	combined	ilium	cancellous	–		5	l.m./Gol	183	74	105	83	l	
Human w/osteo hip fx	>55 yrs	ilium	cancellous	–		5	l.m./Gol	203	70	99	79	l	
Human w/osteo vert fx	>55 yrs	ilium	cancellous	–		5	l.m./Gol	229	66	94	77	l	
Human w/osteo hip/vert fx	>55 yrs	ilium	cancellous	–		5	l.m./Gol	212	69	97	78	l	
Frog	adult	femur	cortical	1°	mid-diap	30–40	l.m.	1,400	27	38	unk	l	Remaggi
Frog	adult	femur	cortical	1°	mid-diap	30–40	l.m.	1,400	27	38	unk	l	et al. [1998]
Chick	adult	femur	cortical	1°	mid-diap	30–40	l.m.	2,800	19	27	unk	l	
Chick	adult	femur	cortical	1°	mid-diap	30–40	l.m.	1,900	23	32	unk	l	
Rabbit	adult	femur	cortical	1° and 2°	mid-diap	30–40	l.m.	2,000	22	32	unk	l	
Rabbit	adult	femur	cortical	1° and 2°	mid-diap	30–40	l.m.	900	33	47	unk	l	
Bovine	adult	MC3	cortical	2°	mid-diap	30–40	l.m.	1,800	24	33	unk	l	
Bovine	adult	MC3	cortical	2°	mid-diap	30–40	l.m.	700	38	54	unk	l	
Horse	adult	MC3	cortical	2°	mid-diap	30–40	l.m.	1,700	24	34	unk	l	
Horse	adult	MC3	cortical	2°	mid-diap	30–40	l.m.	1,100	30	43	unk	l	
Dog	adult	tibia	cortical	2°	mid-diap	30–40	l.m.	2,100	22	31	unk	l	
Dog	adult	tibia	cortical	2°	mid-diap	30–40	l.m.	400	50	71	unk	l	
Man	adult	tibia	cortical	2°	mid-diap	30–40	l.m.	1,000	32	45	unk	l	
Man	adult	tibia	cortical	2°	mid-diap	30–40	l.m.	600	41	58	unk	l	
Female human	<50 yrs	femur	cortical	mostly 2°	mid-diap	100	l.m./fuch	590	41	58	unk	l	Vashishth
	>50 yrs	femur	cortical	mostly 2°	mid-diap	100	l.m./fuch	540	43	61	unk	l	et al. [2000]
Male human	<50 yrs	femur	cortical	mostly 2°	mid-diap	100	l.m./fuch	600	41	58	unk	l	
	>50 yrs	femur	cortical	mostly 2°	mid-diap	100	l.m./fuch	530	43	62	unk	l	
Dog	6 mo–15 yrs	humerus	cortical	mostly 2°	mid-diap	<5	b.f./epif/fuch	775–450	36–47	51–67	unk	l	Frank et al. [2002]
Male human	83 yrs	femur	cortical	resorb 2°	neck	10	b.f./epif/Gol	719	37	53	65	c, l	Power
Male human	83 yrs	femur	cortical	forming 2°	neck	10	b.f./epif/Gol	795	35	50	69	c, l	et al. [2001]
Male human	83 yrs	femur	cortical	quies 2°	neck	10	b.f./epif/Gol	680	38	54	60	c, l	
Female human controls	81 yrs	femur	cortical		neck	10	b.f./epif/Gol	517	44	62	66	c, l	Power
Female human fracture	84 yrs	femur	cortical		neck	10	b.f./epif/Gol	529	43	61	67	c, l	et al. [2002]
Female human	pre-men	illium	cancellous	–		5	l.m./fuch	232	66	93	95	l	Qiu et al. [2002b]
Female human	post-men	illium	cancellous	–		5	l.m./fuch	206	70	99	91	l	
Female human	20–73 yrs	illium	cancellous	–		5	l.m./fuch	227	66	63	unk	l	Qiu et al. [2002a]
Male human	20–25 yrs	rib	cortical	mostly 2°		50	l.m./fuch	848	34	49	unk	l	Qiu et al. [2003]
Female human	50–60	rib	cortical	–		50	l.m./fuch	~825	35	49	unk	l	Qiu et al. [2005]
Sheep	adult	ulna	cortical	2°	mid-diap	100	l.m./fuch	854	34	49	unk	l	Metz et al. [2003]
Turkey	3–4 mo	ulna	cortical	1°	mid-diap	<5	BSE	1,314	28	40	unk	l	Skedros et al. [2003a/b]
Turkey	2 yrs	ulna	cortical	1°	mid-diap	<5	BSE	1,050	31	44	unk	l	

Table 4 (continued)

Species	Age	Bone	Cortical/ cancellous	Histology	Location	Section thick-ness µm	Method/ stain	Ot.Lc.N/ B.Ar n/mm^2	2-D Lc-Lc distance µm	3-D Lc-Lc distance µm	Percent occu-pancy	Cells or lacu-nae	Reference
Mule deer	young fawn	calcaneus	cortical	mostly 2°	mid-diap	<5	BSE	680	38	54	unk	l	
Mule deer	older fawn	calcaneus	cortical	mostly 2°	mid-diap	<5	BSE	666	39	55	unk	l	
Mule deer	subadult	calcaneus	cortical	mostly 2°	mid-diap	<5	BSE	591	41	58	unk	l	
Mule deer	adult	calcaneus	cortical	mostly 2°	mid-diap	<5	BSE	466	46	66	unk	l	
Horse	adult	MC3	cortical	mostly 2°	mid-diap	<5	BSE	475	46	65	unk	l	present study
Horse	adult	radius	cortical	mostly 2°	mid-diap	<5	BSE	511	44	63	unk	l	
Horse	adult	calcaneus	cortical	mostly 2°	mid-diap	<5	BSE	599	41	58	unk	l	Skedros [2005]
Sheep	2 yrs	calcaneus	cortical	mostly 2°	mid-diap	<5	BSE	640	40	56	unk	l	
Elk	adult	calcaneus	cortical	mostly 2°	mid-diap	<5	BSE	681	38	54	unk	l	
Horse (racing)	3.2 yrs	MC3	cortical	1° and 2°	mid-diap	125	epif	589	41	58	unk	c	Gómez et al.
Horse (non-racing)	9.8 yrs	MC3	cortical	1° and 2°	mid-diap	125	epif	552	43	60	unk	c	[2005]

Histology = Specific histology of cortical bone, stated if known; 2-D = 2-dimensional; 3-D = 3-dimensional; cell (c) or lacunae (l) = analysis quantified lacunae versus osteocytes; 1° = primary cortical bone histology not otherwise specified; 2° = secondary cortical bone histology not otherwise specified; unk = unknown; l.m. = light microscope; rib, tib, fem = rib, tibia and femur; mid-diap = mid-diaphysis; h&e = hematoxylin and eosin staining; mo = months; yrs = years; Gol = Goldner staining method; w/osteo = with osteoporotic; vert = vertebral; fx = fracture; fuch = fuchsin staining; resorb = resorbing; quies = quiescent; b.f. = bright field microscopy; epif = epifluorescence microscopy; pre-men = pre-menopausal; post-men = post-menopausal; BSE = backscattered electron imaging.

ies using measures of damage that are representative of complexities of physiologic loading [Joo et al., 2004] may help clarify these issues.

When Ot.Lc.N/B.Ar variations appear to be important for fatigue-related adaptation, they might actually be epiphenomena, reflecting a circumstantial relationship with local histology. This relationship may be strongly dependent on the rate of bone growth, which strongly influences the emergence of initial histologic organization in many bones [de Ricqlès et al., 1991; Stover et al., 1992; Castanet et al., 1996; Currey, 2002; de Margerie, 2002; Mori et al., 2003; de Margerie et al., 2004]. As noted, this conclusion is consistent with studies by Remaggi et al. [1998] and Ferretti et al. [1999] suggesting that biomechanically important relationships are manifest in correlations between animal/bone size and histology (including primary and secondary bone types), and not Ot.Lc.N/B.Ar. This poses a dilemma, namely that horses and other large mammals (e.g., deer and cows) have prevalent fibrolamellar bone (characteristic of rapid bone formation), which is much weaker than lamellar bone (e.g., human secondary osteons) when loaded across the grain [Reilly and Burstein, 1974, 1975]. This behavior appears to be compounded by the stress concentrator effect of osteocyte lacunae. Currey [2003a] offers explanations that might reconcile this apparent anomaly in bones that have fibrolamellar tissue. The first explanation is that fibrolamellar bone is an 'ingenious marrying together' of woven/lamellar bone types; the commingling of these creates a sufficiently strong material. Second, there are a variety of ways that stress can be reduced around osteocyte lacunae and other porous spaces, including changes in the grain of the matrix around these voids; this minimizes their role as stress concentrators [Marotti, 1996; Götzen et al., 2003].

Optimal versus Adequate Arguments for Prioritizing Functions Influenced by Osteocyte Densities

Nutrient/metabolite availability and transport between cells and/or lacunocanalicular spaces may impose important constraints on Ot.Lc.N/B.Ar [Doty and Schofield, 1972; Kelly and Bronk, 1990; Vashishth et al., 2000; Mishra and Knothe Tate, 2003]. In elderly human femoral neck cortices, Power et al. [2002] showed that Ot.Lc.N/B.Ar decreased with increasing distance from Haversian canals. They concluded that this resulted from rate-limited extracellular canalicular fluid flows, i.e. osteocytes farther from canals having less access to nutrients. Modifications in the canalicular network can affect the volume of access channels for load-induced convective flow [Marotti, 1996; Knothe Tate, 2003]. However, significant modifications that may occur during bone growth [Palumbo et al., 1990; Okada et al., 2002; Palumbo et al., 2004] seem only possible in maturity if remodeling occurs. Although we did not study relationships between Ot.Lc.N/B.Ar and nutrient sources, previous data

Table 5. Some parameters that might influence osteocyte densities in diaphyseal/metaphyseal cortices of limb bones

Histologic type (e.g., woven, fibrolamellar, secondary osteons)
Percentage of secondary bone
Remodeling rate
'Envelope' (pericortical, middle, endocortical)
Local rate of osteogenesis (mineral apposition rate) that produced the tissue
Mean tissue age (viable osteocytes *and* Ot.Lc.N/B.Ar decrease with age)
Prevalent/predominant strain mode and other local strain or strain-related characteristics (e.g., fluid flow dynamics)
Size/resolution of 'sensed' entity (i.e. microdamage)
Metabolic requirements/mineral homeostasis
Nutrient delivery[1]

[1] Means/efficiency of nutrient delivery may differ significantly between cancellous and cortical bone. For example in cortical bone, the osteocytes can be in closer proximity to the vascular supply and there is greater importance of fluid flow-mediated delivery driven by functional loading. In contrast, nutrient delivery to trabecular bone is more strongly dependent upon transport/diffusion from the marrow [Fyhrie and Kimura, 1999].

Table 6. Relative influences of some mechanobiological factors or requirements on Ot.Lc.N/B.Ar

Histology/tissue constraints
Microdamage detection
Social/communication
Nutrition
Metabolism

Listed in order of putative importance. Top = most important; bottom = least important.

suggest that Ot.Lc.N/B.Ar would *not* be greatly limited by nutrient delivery if tissue strains pump nutrients to cells. Martin [2003] notes strong evidence that nutrient transport cannot be accomplished by diffusion through the calcified matrix or through canaliculi, but must involve such convective transport [Knothe Tate et al., 2000; Knothe Tate, 2001]. This '… suggests that the very existence of osteocytes in the bone matrix depends on substantial tissue deformations during functional loading' [Martin, 2003, p. 105]. Consequently, Martin [2003, p. 105] concludes that:

> If one assumes that keeping the skeleton light (relative to the size of the animal) has often conferred significant adaptive advantages during vertebrate evolution, then it follows that there have been pressures to push functional strains in bones upward to the point that fatigue damage is an ever present phenomenon. In this scenario, remodeling provides a means to deal with this problem by constantly removing the damage as it occurs. In the same context, osteocytes hypothetically evolved both as strain sensors (to keep the skeleton light and functional strains high, but not too high) and fatigue damage sensors able to direct the removal of damage as needed.

If this view is correct, then, among parameters that influence osteocyte density, the influence of nutrient delivery per se should be relatively negligible because it is intimately linked to fluid flow produced by strain (tables 5, 6).

Considering relationships between osteocyte densities and their putative biomechanical functions, Fyhrie and Kimura [1999] applied Liebig's 'Law of the Minima' [Lotka, 1956; Hall, 2000] which states that the growth of an organism is dependent on the amount of essential material available in minimum quantity. Considering the relationship between bone volume fraction and the supply and demand of metabolites, they argue that osteocyte densities may be selected such that they approach a minimum density for satisfying various mechanobiological requirements. Because competing demands can be different between species, histologic types and skeletal locations, an 'optimum' Ot.Lc.N/B.Ar probably does not exist, and Ot.Lc.N/B.Ar in a bone or bone region is probably a compromise, falling in an 'adequate range' (table 5). Assuming that rates of cell recruitment, not nutritional demands, determine local osteocyte density, then it is theorized that broad interspecies differences (table 4) are strongly influenced by the density of the 'operational' network required for strain and fatigue microdamage detection within specific histologic types (table 6). These histologic types, although developmentally constrained, are probably ultimately 'determined' by fatigue-related requirements. However, the emergence of Ot.Lc.N/B.Ar can be influenced by a variety of factors, and this is especially obvious when comparing primary versus secondary bone formation (i.e. modeling versus remodeling). For example, as shown in figure 7, various stimuli can influence the rate of osteoblast recruitment and their percent survival as osteocytes, possibly accounting for different cell densities in primary versus secondary bone. Consequently, since modeling results in net bone gain, and remodeling typically results in net bone loss, the older or more highly remodeled the tissue, the lower the correlation between Ot.Lc.N/B.Ar and bone mass.

Conclusion

Although osteocytes probably have multifactorial functions, it is not known to what degree these functions are influenced by differences in their densities. Although we have considered our results in the context of proven or hypothesized mechanobiological functions, we found little or no evidence that the number of osteocyte lacunae has a functional role in mechanotransduction pathways that lead to remodeling in the bones of the current study. In view of other investigators' findings that have shown that at least a portion of remodeling is targeted, we presume that other mechanotransduction pathways predominate in the equine radius and MC3. As discussed in our companion study [Skedros 2005], these can include innervation of bone and changes in the dendritic processes of osteocytes within canaliculi that are not associated with osteocyte death and changes in osteocyte lacunar density. However, we were only able to test some hypotheses indirectly; therefore, care must be taken when considering the present data in these contexts. This study examined only mid-diaphyses of two bones from one species; hence, much work is needed to further examine the various putative osteocyte functions and how they are influenced by cell-cell and cell-matrix interactions in various tissue types, bones and species. Nevertheless, we found relatively uniform osteocyte lacuna densities between regions with highly non-uniform strain-related environments and markedly heterogeneous material organization. It is not known if these relatively uniform densities are associated with cell level 'adaptations' that do not require modeling/remodeling events. Whether or not some functions are mediated by 'volume transmission' and others by 'wiring transmission' are also compelling possibilities about how osteocytes function as 'operational' networks. It is clear that the configuration of the osteocytic lacunocanalicular network is well suited for perceiving mechanical and mechanically related environmental stimuli and for influencing remodeling/modeling activities and the targeted repair of microdamage. Although osteocyte densities might vary in accordance with requirements for social/communication, mechanosensory, and nutrition/metabolism requirements/constraints, the mechanisms that govern the production and maintenance of species/site-specific histogenesis might be the most important factors governing the distribution of these cells. In turn, these tissue level 'adaptations' appear to require strain and fatigue damage sensors, which may be one function of osteocyte networks.

Acknowledgments

This study was supported by grants from the National Science Foundation, the Department of Veteran Affairs Medical Research Funds, and Orthopaedic Research and Education Foundation grant No. 01-024. The authors thank Kevin Dietch, Ebstasam Attaya and Milena Zirovich for their technical work, Roy Bloebaum for laboratory support, Mark Mason for his technical work and assistance with the statistical analyses, Kerry Matz for the illustrations, and Christian Sybrowsky, Scott Sorenson, Teri Rosenbaum, and anonymous reviewers for their critical reviews of the manuscript.

References

Aarden, E.M., E.H. Burger, P.J. Nijweide (1994) Function of osteocytes in bone. J Cell Biochem *55:* 287–299.

Alford, A.I., C.R. Jacobs, H.J. Donahue (2003) Oscillating fluid flow regulates gap junction communication in osteocytic MLO-Y4 cells by an ERK1/2 MAP kinase-dependent mechanism small star, filled. Bone *33:* 64–70.

Batson, E.L., G.C. Reilly, J.D. Currey, D.S. Balderson (2000) Postexcercise and positional variation in mechanical properties of the radius in young horses. Equine Vet J *32:* 95–100.

Baud, C.A., E. Auil (1971) Osteocyte differential count in normal human alveolar bone. Acta Anat *78:* 287–299.

Bentolila, V., T.M. Boyce, D.P. Fyhrie, R. Drumb, T.M. Skerry, M.B. Schaffler (1998) Intracortical remodeling in adult rat long bones after fatigue loading. Bone *23:* 275–281.

Bloebaum, R.D., J.G. Skedros, E.G. Vajda, K.N. Bachus, B.R. Constantz (1997) Determining mineral content variations in bone using backscattered electron imaging. Bone *20:* 485–490.

Bouvier, M., W.L. Hylander (1981) Effect of bone strain on cortical bone structure in macaques *(Macaca mulatta).* J Morphol *167:* 1–12.

Bowman, B.M., S.C. Miller (2001) Skeletal adaptations during mammalian reproduction. J Musculoskel Neuron Interact *1:* 347–355.

Boyde, A., C.M. Riggs (1990) The quantitative study of the orientation of collagen in compact bone slices. Bone *11:* 35–39.

Bromage, T.G., H.M. Goldman, S.C. McFarlin, J. Warshaw, A. Boyde, C.M. Riggs (2003) Circularly polarized light standards for investigations of collagen fiber orientation in bone. Anat Rec B New Anat *274:* 157–168.

Burger, E.H., J. Klein-Nulend (1999) Mechanotransduction in bone – Role of the lacunocanalicular network. FASEB J *13:* S101–S112.

Burger, E.H., J. Klein-Nulend, T.H. Smit (2003) Strain-derived canalicular fluid flow regulates osteoclast activity in a remodelling osteon – A proposal. J Biomech *36:* 1453–1459.

Butler, W.T. (1989) The nature, significance of osteopontin. Connect Tissue Res *23:* 123–136.

Canè, V., G. Marotti, G. Volpi, D. Zaffe, S. Palazzini, F. Remaggi, M.A. Muglia (1982) Size and density of osteocyte lacunae in different regions of long bones. Calcif Tissue Int *34:* 558–563.

Carter, D.R. (1987) Mechanical loading history and skeletal biology. J Biomech *20:* 1095–1109.

Carter, D.R., G.S. Beaupré (2001) Skeletal Function and Form. Cambridge, Cambridge University Press, pp 138–160.

Carter, D.R., W.C. Hayes (1976) Fatigue life of compact bone. 1. Effects of stress amplitude, temperature and density. J Biomech *9:* 27–34.
Castanet, J., A. Grandin, A. Abourachid, A. de Ricqlès (1996) Expression of growth dynamic in the structure of the periosteal bone in *Anas platyrhynchos.* C R Acad Sci III *319:* 301–308.
Cowin, S.C., L. Moss-Salentijn, M.L. Moss (1991) Candidates for the mechanosensory system in bone. J Biomech Eng *113:* 191–197.
Cullinane, D.M. (2002) The role of osteocytes in bone regulation: mineral homeostasis versus mechanoreception. J Musculoskel Neuron Interact *2:* 242–244.
Currey, J.D. (1962) Stress concentrations in bone. Quart J Microsc Sci *103:* 111–133.
Currey, J.D. (1964) Some effects of aging in human haversian systems. J Anat Lond *98:* 69–75.
Currey, J.D. (2002) Bones: Structure and Mechanics. Princeton, Princeton University Press, p 436.
Currey, J.D. (2003) The many adaptations of bone. J Biomech *36:* 1487–1495.
de Margerie, E. (2002) Laminar bone as an adaptation to torsional loads in flapping flight. J Anat *201:* 521–526.
de Margerie, E., J.P. Robin, D. Verrier, J. Cubo, R. Groscolas, J. Castanet (2004) Assessing a relationship between bone microstructure and growth rate: a fluorescent labelling study in the king penguin chick *(Aptenodytes patagonicus).* J Exp Biol *207:* 869–879.
de Ricqlès, A., F.J. Meunier, L. Castanet, H. Francillon-Vieillot (1991) Comparative microstructure of bone; in Hall, B.K. (ed): Bone. Boca Raton, CRC Press, vol 3: Bone Matrix and Bone Specific Products, pp 1–78.
Donahue, H.J. (1998) Gap junctional intercellular communication in bone: a cellular basis for the mechanostat set point. Calcif Tissue Int *62:* 85–88.
Donahue, H.J. (2000) Gap junctions and biophysical regulation of bone cell differentiation. Bone *26:* 417–422.
Doty, S.B. (1981) Morphological evidence of gap junctions between bone cells. Calcif Tissue Int *33:* 509–512.
Doty, S.B., B.H. Schofield (1972) Electron microscopic localization of hydrolytic enzymes in osteoclasts. Histochem J *4:* 245–258.
Duncan, R.L., C.H. Turner (1995) Mechanotransduction and functional response of bone to mechanical strain. Calcif Tissue Int *57:* 344–358.
Ehrlich, P.J., B.S. Noble, H.L. Jessop, H.Y. Stevens, J.R. Mosley, L.E. Lanyon (2002) The effect of in vivo mechanical loading on estrogen receptor alpha expression in rat ulnar osteocytes. J Bone Miner Res *17:* 1646–1655.
Emmanual, J., C. Hornbeck, R.D. Bloebaum (1987) A polymethyl methacrylate method for large specimens of mineralized bone with implants. Stain Tech *62:* 401–410.
Erlebacher, A., E.H. Filvaroff, J.Q. Ye, R. Derynck (1998) Osteoblastic responses to TGF-beta during bone remodeling. Mol Biol Cell *9:* 1903–1918.
Ferretti, M., M.A. Muglia, F. Remaggi, V. Canè, C. Palumbo (1999) Histomorphometric study on the osteocyte lacuno-canalicular network in animals of different species. 2. Parallel-fibered and lamellar bones. Ital J Anat Embryol *104:* 121–131.
Frank, J.D., M. Ryan, V.L. Kalscheur, C.P. Ruaux-Mason, R.R. Hozak, P. Muir (2002) Aging and accumulation of microdamage in canine bone. Bone *30:* 201–205.
Frost, H.M. (1960) In vivo osteocyte death. Am J Orthop *42-A:* 138–143.
Frost, H.M. (1998) A brief review for orthopedic surgeons: fatigue damage (microdamage) in bone (its determinants and clinical implications). J Orthop Sci *3:* 272–281.
Fyhrie, D.P., J.H. Kimura (1999) NACOB presentation Keynote lecture. Cancellous bone biomechanics. North American Congress on Biomechanics. J Biomech *32:* 1139–1148.
Gómez, T.M., J.G. Barrett, S.J. Sample, C.L. Radtke, V.L. Kalscheur, Y. Lu, M.D. Markel, E.M. Santschi, M.C. Scollay, P. Muir (2005) Up-regulation of site-specific remodeling without accumulation of microcracking and loss of osteocytes. Bone, in press.
Götzen, N., A.R. Cross, P.G. Ifju, A.J. Rapoff (2003) Understanding stress concentrations about a nutrient foramen. J Biomech *36:* 1511–1521.
Gross, T.S., J.L. Edwards, K.J. McLeod, C.T. Rubin (1997) Strain gradients correlate with sites of periosteal bone formation. J Bone Miner Res *12:* 982–988.
Gross, T.S., K.J. McLeod, C.T. Rubin (1992) Characterizing bone strain distribution in vivo using three triple rosette strain gauges. J Biomech *25:* 1081–1087.
Hall, C.H. (2000) Laws and Models: Science, Engineering and Technology. Boca Raton, CRC press.
Heaney, R.P. (2003) How does bone support calcium homeostasis? Bone *33:* 264–268.
Heino, T.J., T.A. Hentunen, H.K. Vaananen (2002) Osteocytes inhibit osteoclastic bone resorption through transforming growth factor-beta: enhancement by estrogen. J Cell Biochem *85:* 185–197.
Hiller, L.P., S.M. Stover, V.A. Gibson, J.C. Gibeling, C.S. Prater, S.J. Hazelwood, O.C. Yeh, R.B. Martin (2003) Osteon pullout in the equine third metacarpal bone: effects of ex vivo fatigue. J Orthop Res *21:* 481–488.
Hobdell, M.H., C.E. Howe (1971) Variation in bone matrix volume associated with osteocyte lacunae in mammalian and reptilian bone. Isr J Med Sci *7:* 492–493.
Huiskes, R. (2000) If bone is the answer, then what is the question? J Anat *197:* 145–156.
Joo, W., K.J. Jepsen, D.T. Davy (2004) Complex cross-modal effects of damage on cortical bone properties. Trans Orthop Res Soc *29:* 515.
Jowsey, J. (1966) Studies of Haversian systems in man and some animals. J Anat *100:* 857–864.
Judex, S., T.S. Gross, R.C. Bray, R.F. Zernicke (1997a) Adaptation of bone to physiological stimuli. J Biomech *30:* 421–429.
Judex, S., T.S. Gross, R.F. Zernicke (1997b) Strain gradients correlate with sites of exercise-induced bone-forming surfaces in adult skeleton. J Bone Miner Res *12*: 1737–1745.
Kalmey, J.K., C.O. Lovejoy (2002) Collagen fiber orientation in the femoral necks of apes and humans: do their histological structures reflect differences in locomotor loading? Bone *31:* 327–332.
Karsdal, M.A., T.A. Andersen, L. Bonewald, C. Christiansen (2004) Matrix metalloproteinases (MMPs) safeguard osteoblasts from apoptosis during transdifferentiation into osteocytes: MT1-MN maintains osteocyte viability. DNA Cell Biol *23:* 155–156.
Kelly, P.J. (1983) Pathways of transport in bone; in Geiger, S.R. (ed): Handbook of Physiology. The Cardiovascular System, pt 1: Peripheral Circulations and Organ Blood Flow. Bethesda, American Physiological Society, pp 371–396.
Kelly, P.J., J.T. Bronk (1990) Venous pressure and bone formation. Microvasc Res *39:* 364–375.
Kim, D.G., J.B. Brunski, D.P. Nicolella (2004) Microstrain fields in cortical bone in uniaxial tension. Trans Orthop Res Soc *29:* 493.
Knothe Tate, M. L. (2001) Mixing mechanisms and net solute transport in bone. Ann Biomed Eng *29:* 810–811.
Knothe Tate, M.L. (2003) 'Whither flows the fluid in bone?' An osteocyte's perspective. J Biomech *36:* 1409–1424.
Knothe Tate, M.L., R. Steck, M.R. Forwood, P. Niederer (2000) In vivo demonstration of load-induced fluid flow in the rat tibia and its potential implications for processes associated with functional adaptation. J Exp Biol *203:* 2737–2745.
Kornblum, S.S., P.J. Kelly (1964) The lacunae and haversian canals in tibial cortical bone from ischemic and non-ischemic limbs. A comparative microradiographic study. J Bone Joint Surg Am *46:* 797–810.
Lanyon, L.E. (1993) Osteocytes, strain detection, bone modeling and remodeling. Calcif Tissue Int *53(suppl 1):* S102–S106; discussion S106–S107.
Lanyon, L.E., S. Bourn (1979) The influence of mechanical function on the development and remodeling of the tibia: An experimental study in sheep. J Bone Joint Surg *61-A:* 263–273.
Lotka, A.J. (1956) Elements of Mathematical Biology. New York, Dover.
Marotti, G. (1963) Quantitative studies on bone reconstruction. 1. The reconstruction in homotypic shaft bones. Acta Anat *52:* 291–333.
Marotti, G. (1996) The structure of bone tissues and the cellular control of their deposition. Ital J Anat Embryol *101:* 25–79.
Marotti, G. (2000) The osteocyte as a wiring transmission system. J Musculoskel Neuron Interact *1:* 133–136.
Marotti, G., V. Cane, S. Palazzini, C. Palumbo (1990) Structure-function relationships in the osteocyte. Ital J Miner Electrolyte Metab *4:* 93–106.
Martin, R.B. (2000) Toward a unifying theory of bone remodeling. Bone *26:* 1–6.

Martin, R.B. (2003) Fatigue microdamage as an essential element of bone mechanics and biology. Calcif Tissue Int *73:* 101–107.
Martin, R.B., D.B. Burr (1989) Structure, Function and Adaptation of Compact Bone. New York, Raven Press, pp 1–275.
Martin, R.B., D.B. Burr, N.A. Sharkey (1998) Skeletal Tissue Mechanics. New York, Springer, pp 1–392.
Martin, R.B., P.V. Mathews, S.T. Lau, V.A. Gibson, S.M. Stover (1996) Collagen fiber organization is related to mechanical properties and remodeling in equine bone. A comparison of two methods. J Biomech *29:* 1515–1521.
Mason, M.W., J.G. Skedros, R.D. Bloebaum (1995) Evidence of strain-mode-related cortical adaptation in the diaphysis of the horse radius. Bone *17:* 229–237.
McCreadie, B.R., S.J. Hollister (1997) Strain concentrations surrounding an ellipsoid model of lacunae and osteocytes. Comput Methods Biomech Biomed Engin *1:* 61–68.
Metz, L.N., B. Martin, S. Turner (2003) Osteocyte density affects osteon refilling in basic multicellular units. Trans Orthop Res Soc *28:* poster No 0367.
Mishra, S., M.L. Knothe Tate (2003) Effect of lacunocanalicular architecture on hydraulic conductance in bone tissue: implications for bone health and evolution. Anat Rec A Discov Mol Cell Evol Biol *273:* 752–762.
Mori, R., T. Kodaka, T. Sano, N. Yamagishi, M. Asari, Y. Naito (2003) Comparative histology of the laminar bone between young calves and foals. Cells Tissues Organs *175:* 43–50.
Mori, S., D.B. Burr (1993) Increased intracortical remodeling following fatigue damage. Bone *14:* 103–109.
Mosley, J.R., L.E. Lanyon (1998) Strain rate as a controlling influence on adaptive modeling in response to dynamic loading of the ulna in growing male rats. Bone *23:* 313–318.
Mullender, M.G., R. Huiskes (1995) Proposal for the regulatory mechanism of Wolff's law. J Orthop Res *13:* 503–512.
Mullender, M.G., R. Huiskes (1997) Osteocytes and bone lining cells: which are the best candidates for mechano-sensors in cancellous bone? Bone *20*: 527–532.
Mullender, M.G., R. Huiskes, H. Versleyen, P. Buma (1996a) Osteocyte density and histomorphometric parameters in cancellous bone of the proximal femur in five mammalian species. J Ortho Res *14:* 972–979.
Mullender, M.G., D.D. van der Meer, R. Huiskes, P. Lips (1996b) Osteocyte density changes in aging and osteoporosis. Bone *18:* 109–113.
Nalla, R.K., J.S. Stolken, J.H. Kinney, R.O. Ritchie (2005) Fracture in human cortical bone: local fracture criteria and toughening mechanisms. J Biomech *38:* 1517–1525.
Nicolella, D.P., J. Lankford, D.J. Jepsen (1997) Correlation of physical damage development with microstructure and strain localization in bone. Am Soc Mech Eng *35:* 311–312.
Noble, B.S., N. Peet, H.Y. Stevens, A. Brabbs, J.R. Mosley, G.C. Reilly, J. Reeve, T.M. Skerry, L.E. Lanyon (2003) Mechanical loading: biphasic osteocyte survival and targeting of osteoclasts for bone destruction in rat cortical bone. Am J Physiol Cell Physiol *284:* C934–C943.
Noble, B.S., J. Reeve (2000) Osteocyte function, osteocyte death and bone fracture resistance. Mol Cell Endocrinol *159:* 7–13.
Okada, S., S. Yoshida, S.H. Ashrafi, D.E. Schraufnagel (2002) The canalicular structure of compact bone in the rat at different ages. Microsc Microanal *8:* 104–115.
Palumbo, C., M. Ferretti, G. Marotti (2004) Osteocyte dendrogenesis in static and dynamic bone formation: an ultrastructural study. Anat Rec A Discov Mol Cell Evol Biol *278:* 474–480.
Palumbo, C., S. Palazzini, D. Zaffe, G. Marotti (1990) Osteocyte differentiation in the tibia of newborn rabbit: an ultrastructural study of the formation of cytoplasmic processes. Acta Anat *37:* 350–358.
Parfitt, A.M. (1987) Bone and plasma calcium homeostasis. Bone *8(suppl 1):* S1–S8.
Parfitt, A.M. (1993a) Bone age, mineral density, and fatigue damage. Calcif Tissue Int *53*(*suppl 1*): S82–S85; discussion S85–S86.
Parfitt, A.M. (1993b) Calcium homeostasis; in Mundy, G.R., T.J. Martin (eds): Physiology and Pharmacology of Bone. Berlin, Springer, pp 1–65.
Parfitt, A.M. (2001) The bone remodeling compartment: a circulatory function for bone lining cells. J Bone Miner Res *16:* 1583–1585.
Parfitt, A.M. (2003) Misconceptions (3): calcium leaves bone only by resorption and enters only by formation. Bone *33:* 259–263.
Pavalko, F.M., N.X. Chen, C.H. Turner, D.B. Burr, S. Atkinson, Y.F. Hsieh, J. Qui, R.L. Duncan (1998) Fluid shear-induced mechanical signaling in MC3T3-E1 osteoblasts requires cytoskeleton-integrin interactions. Am J Physiol *275:* C1591–C1601.
Portigliatti Barbos, M., P. Bianco, A. Ascenzi, A. Boyde (1984) Collagen orientation in compact bone. 2. Distribution of lamellae in the whole of the human femoral shaft with reference to its mechanical properties. Metab Bone Dis Relat Res *5:* 309–315.
Power, J., N. Loveridge, N. Rushton, M. Parker, J. Reeve (2002) Osteocyte density in aging subjects is enhanced in bone adjacent to remodeling haversian systems. Bone *30:* 859–865.
Power, J., B.S. Noble, N. Loveridge, K.L. Bell, N. Rushton, J. Reeve (2001) Osteocyte lacunar occupancy in the femoral neck cortex: an association with cortical remodeling in hip fracture cases and controls. Calcif Tissue Int *69:* 13–19.
Prendergast, P.J., R. Huiskes (1995) The biomechanics of Wolff's law: recent advances. Ir J Med Sci *164:* 152–154.
Qiu, S., D.P. Fyhrie, S. Palnitkar, D.S. Rao (2003) Histomorphometric assessment of haversian canal and osteocyte lacunae in different-sized osteons in human rib. Anat Rec *727A:* 520–525.
Qiu, S., D.S. Rao, D.P. Fyhrie, S. Palnitkar, A.M. Parfitt (2005) The morphological association between microcracks and osteocyte lacunae in human cortical bone. Bone *37:* 10–15.
Qiu, S., D. S. Rao, S. Palnitkar, A.M. Parfitt (2002a) Relationship between osteocyte density and bone formation rate in human cancellous bone. Bone *31:* 709–711.
Qiu, S., D.S. Rao, S. Palnitkar, A.M. Parfitt (2002b) Age and distance from the surface but not menopause reduce osteocyte density in human cancellous bone. Bone *31:* 313–318.
Reilly, D.T., A.H. Burstein (1974) The mechanical properties of cortical bone. J Bone Joint Surg Am *56:* 1001–1022.
Reilly, D.T., A.H. Burstein (1975) The elastic and ultimate properties of compact bone tissue. J Biomech *8:* 393–405.
Reilly, G.C. (2000) Observations of microdamage around osteocyte lacunae in bone. J Biomech *33:* 1131–1134.
Reilly, G.C., J.D. Currey (1999) The development of microcracking and failure in bone depends on the loading mode to which it is adapted. J Exp Biol *202:* 543–552.
Reilly, G.C., J.D. Currey, A. Goodship (1997) Exercise of young thoroughbred horses increases impact strength of the third metacarpal bone. J Orthop Res *15:* 862–868.
Remaggi, F., V. Canè, C. Palumbo, M. Ferretti (1998) Histomorphometric study on the osteocyte lacuno-canalicular network in animals of different species. 1. Woven-fibered and parallel-fibered bones. Ital J Anat Embryol *103:* 145–155.
Riggs, C.M., L.E. Lanyon, A. Boyde (1993) Functional associations between collagen fibre orientation and locomotor strain direction in cortical bone of the equine radius. Anat Embryol *187:* 231–238.
Robling, A.G., C.H. Turner (2002) Mechanotransduction in bone: genetic effects on mechanosensitivity in mice. Bone *31:* 562–569.
Rodionova, N.V., V.S. Oganov, N.V. Zolotova (2002) Ultrastructural changes in osteocytes in microgravity conditions. Adv Space Res *30:* 765–770.
Rubin, C., S. Judex, M. Hadjiargrou (2002) Skeletal adaptation to mechanical stimuli in the absence of formation or resorption of bone. J Musculoskel Neuron Interact *2:* 264–267.
Rubinacci, A., M. Covini, C. Bisogni, I. Villa, M. Galli, C. Palumbo, M. Ferretti, M.A. Muglia, G. Marotti (2002) Bone as an ion exchange system: evidence for a link between mechanotransduction and metabolic needs. Am J Physiol Endocrinol Metab *282:* E851–E864.
Schneider, R.K., D.W. Milne, A.A. Gabel, J.J. Groom, L.R. Bramlage (1982) Multidirectional in vivo strain analysis of the equine radius and tibia during dynamic loading with and without a cast. Am J Vet Res *43:* 1541–1550.
Singh, I.J., E.A. Tonna, C.P. Gandel (1974) A comparative histological study of mammalian bone. J Morph *144:* 421–438.

Skedros, J.G. (1994a) Collagen fiber orientation in skeletal tension/compression systems: a potential role of variant strain stimuli in the maintenance of cortical bone organization. J Bone Miner Res *9:* S251.
Skedros, J.G. (2001a) Collagen fiber orientation: a characteristic of strain-mode-related regional adaptation in cortical bone. Bone *28:* S110–S111.
Skedros, J.G. (2005) Osteocyte lacuna population densities in sheep, elk, and horse calcanei. Cells Tissues Organs *181:* 23–37.
Skedros, J.G., R.D. Bloebaum, K.N. Bachus, T.M. Boyce (1993a) The meaning of graylevels in backscattered electron images of bone. J Biomed Mater Res *27:* 47–56.
Skedros, J.G., R.D. Bloebaum, K.N. Bachus, T.M. Boyce, B. Constantz (1993b) Influence of mineral content and composition of graylevels in backscattered electron images of bone. J Biomed Mater Res *27:* 57–64.
Skedros, J.G., M.R. Dayton, C.L. Sybrowsky, R.D. Bloebaum, K.N. Bachus (2003a) Are uniform regional safety factors an objective of adaptive modeling/remodeling in cortical bone? J Exp Biol *206:* 2431–2439.
Skedros, J.G., K.J. Hunt (2004a) Does the degree of laminarity mediate site-specific differences in collagen fiber orientation in primary bone? An evaluation in the turkey ulna diaphysis. J Anat *205:* 121–134.
Skedros, J.G., K.J. Hunt, R.D. Bloebaum (2004b) Relationships of loading history and structural and material characteristics of bone: development of the mule deer calcaneus. J Morphol *259:* 281–307.
Skedros, J.G., K.J. Hunt, M.R. Dayton, R.D. Bloebaum, K.N. Bachus (2001b) Relative contributions of material characteristics to failure properties of cortical bone in strain-mode-specific loading: implications for fragility in osteoporosis and aging. Trans Am Soc Biomech *25:* 215–216.
Skedros, J.G., K.J. Hunt, P.E. Hughes, H. Winet (2003c) Ontogenetic and regional morphologic variations in the turkey ulna diaphysis: implications for functional adaptation of cortical bone. Anat Rec A Discov Mol Cell Evol Biol *273:* 609–629.
Skedros, J.G., K.J. Hunt, C.L. Sybrowsky (2002) Ontogenetic development of the ovine calcaneus: a model for examining the relative contributions of genetic, epigenetic, and extra-genetic stimuli. J Bone Miner Res *17:* S330.
Skedros, J.G., T.Y. Kuo (1999) Ontogenetic changes in regional collagen fiber orientation suggest a role for variant strain stimuli in cortical bone construction. J Bone Miner Res *14:* S441.
Skedros, J.G., M.W. Mason, R.D. Bloebaum (1994b) Differences in osteonal micromorphology between tensile and compressive cortices of a bending skeletal system: indications of potential strain-specific differences in bone microstructure. Anat Rec *239:* 405–413.
Skedros, J. G., M. W. Mason, R.D. Bloebaum (2001b) Modeling and remodeling in a developing artiodactyl calcaneus: a model for evaluating Frost's mechanostat hypothesis and its corollaries. Anat Rec *263:* 167–185.
Skedros, J.G., M.W. Mason, M.C. Nelson, R.D. Bloebaum (1996) Evidence of structural and material adaptation to specific strain features in cortical bone. Anat Rec *246:* 47–63.
Skedros, J.G., S.C. Su, R.D. Bloebaum (1997) Biomechanical implications of mineral content and microstructural variations in cortical bone of horse, elk, and sheep calcanei. Anat Rec *249:* 297–316.
Skedros, J.G., C.L. Sybrowsky, M.R. Dayton, R.D. Bloebaum, K.N. Bachus (2003c) The role of osteocyte lacuna population density on the mechanical properties of cortical bone. Trans Orthop Res Soc *28:* 414.
Sobelman, O.S., J.C. Gibeling, S.M. Stover, S.J. Hazelwood, O.C. Yeh, D.R. Shelton, R.B. Martin (2004) Do microcracks decrease or increase fatigue resistance in cortical bone? J Biomech *37:* 1295–1303.
Srinivasan, S., T.S. Gross (2000) Canalicular fluid flow induced by bending of a long bone. Med Eng Phys *22:* 127–133.
Starkebaum, W. (1979) Microelectrode studies of stress-generated potentials in four-point bending of bone. J Biomed Mater Res *13:* 729–751.
Staub, J.F., P. Tracqui, S. Lausson, G. Milhaud, A.M. Perault-Staub (1989) A physiologic view of in vivo calcium dynamics: the regulation of a nonlinear self-organized system. Bone *10:* 77–86.
Stout, S., D.J. Simmons (1979) Use of histology in ancient bone research. Yearb Phys Anthropol *22:* 228–249.
Stover, S.M., R.R. Pool, R.B. Martin, J.P. Morgan (1992) Histological features of the dorsal cortex of the third metacarpal bone mid-diaphysis during postnatal growth in thoroughbred horses. J Anat *181:* 455–469.
Takano, Y., C.H. Turner, I. Owan, R.B. Martin, S.T. Lau, M.R. Forwood, D.B. Burr (1999) Elastic anisotropy and collagen orientation of osteonal bone are dependent on the mechanical strain distribution. J Orthop Res *17:* 59–66.
Talmage, R.V., G.E. Lester, P.F. Hirsch (2000) Parathyroid hormone and plasma calcium control. J Musculoskel Neuron Interact *1:* 121–126.
Tami, A.E., P. Nasser, O. Verborgt, M. Schaffler, M.L. Knothe Tate (2002) The role of interstitial flow in the remodeling response to fatigue loading. J Bone Miner Res *17:* 2030–2037.
Taylor, D. (2000) Scaling effects in the fatigue strength of bones from different animals. J Theor Biol *206:* 299–306.
Tazawa, K., K. Hoshi, S. Kawamoto, M.M. Tanaka, S. Ejiri, H. Ozawa (2004) Osteocytic osteolysis observed in rats to which parathyroid hormone was continuously administered. J Bone Miner Metab *22*: 524–529.
Terai, K., T. Takano-Yamamoto, Y. Ohba, K. Hiura, M. Sugimoto, M. Sato, H. Kawahata, N. Inaguma, Y. Kitamura, S. Nomura (1999) Role of osteopontin in bone remodeling caused by mechanical stress. J Bone Miner Res *14:* 839–849.
Turner, C.H., A.G. Robling, R.L. Duncan, D.B. Burr (2002) Do bone cells behave like a neuronal network? Calcif Tissue Int *70:* 435–442.
Vashishth, D., G. Gibson, J. Kimura, M.B. Schaffler, D.P. Fyhrie (2002) Determination of bone volume by osteocyte population. Anat Rec *267:* 292–295.
Vashishth, D., O. Verborgt, G. Divine, M. Schaffler, D.P. Fyhrie (2000) Decline in osteocyte lacunar density in human cortical bone is associated with accumulation of microcracks with age. Bone *26:* 375–380.
Verborgt, O., G.J. Gibson, M.B. Schaffler (2000) Loss of osteocyte integrity in association with microdamage and bone remodeling after fatigue in vivo. J Bone Miner Res *15:* 60–67.
Weinbaum, S., S.C. Cowin, Y. Zeng (1994) A model for the excitation of osteocytes by mechanical loading-induced bone fluid shear stresses. J Biomech *27:* 339–360.
Weinbaum, S., P. Guo, L. You (2001) A new view of mechanotransduction and strain amplification in cells with microvilli and cell processes. Biorheology *38:* 119–142.
Wong, S.Y.P., R.A. Evans, C. Needs, C.R. Dunstan, E. Hills (1985) The effect of age on bone composition and viability in the femoral head. J Bone Joint Surg *67:* 274–283.
Wong, S.Y.P., R.A. Evans, C. Needs, C.R. Dunstan, E. Hills, J. Garvan (1987) The pathogenesis of osteoarthritis of the hip. Clin Orthop Relat Res *214:* 305–312.
Yellowley, C.E., Z. Li, Z. Zhou, C.R. Jacobs, H.J. Donahue (2000) Functional gap junctions between osteocytic and osteoblastic cells. J Bone Miner Res *15:* 209–217.
Yeni, Y.N., D. Vashishth, D.P. Fyhrie (2001) Estimation of bone matrix apparent stiffness variation caused by osteocyte lacunar size and density. J Biomech Eng *123:*10–17.